TÉCNICO LISBOA

Inhibition formalisms of Sb catalysis in BHET-glycol systems

Pedro de Oliveira Abi Rached

Thesis to obtain the Master of Science Degree in

Chemical Engineering

Supervisors:

Dr. Adrien Mekki-Berrada

Prof. Dr. Maria do Rosário Gomes Ribeiro

Examination Committee

Chairperson: Prof. Dr. Maria Cristina De Carvalho Silva Fernandes

Supervisor: Dr. Adrien Mekki-Berrada

Members of the Committee: Prof. Dr. Maria Filipa Gomes Ribeiro

November 2022

This work was done in collaboration with

Acknowledgements

The realisation and completion of the current work would not have been possible without the crucial help, support and motivation from some extremely important people in my life.

Foremost, I would like to express my sincere gratitude to my parents, Maria Cristina Marino de Oliveira and Roberto Abi Rached, who have followed and guided me with love for over twenty-three years and taught me what perseverance and hard-work look like. I owe them all the opportunities I have ever had and all the accomplishments I have ever achieved in my life.

I would like to express my most sincere gratitude and appreciation to both of my supervisors from IFPEN, Dr. Adrien Mekki-Berrada and Dr. Nicolas Vin, and to my supervisor from IST, Prof. Dr. Maria do Rosário Ribeiro, for the precious knowledge and expertise that they have transmitted me during my internship and beyond. Their continuous and enduring patience, encouragement and feedback were my main guidance throughout all stages of my internship, from the research to the writing process, and were what allowed me to obtain results that I was proud of.

I would also like to extend my gratitude to all people at IFPEN who were involved in my work. I wish to thank Marie-Olive Clarte, Lucas Darley, Khaled Belhaddad, Severine Artero and Karine Gaillard, for all their help with my laboratory work and the instructions they gave me when I first arrived at IFPEN. I also wish to thank Maeva Fieu, for her expertise in the analytical techniques needed for processing the experimental results of my internship, and for always kindly answering any questions I had. Finally, I also wish to thank Dr. Frédéric Favre and Joseph Muller for their help and sharing of skills and practices.

Finally, I would like to thank the members of the jury, Prof. Dr. Cristina Fernandes and Prof. Dr. Filipa Ribeiro, for letting my defense be an enjoyable moment, with great questions and suggestions for improving.

Never be satisfied with less than your very best effort. If you strive for the top and miss, you'll still 'beat the pack'

— Gerald R. Ford —

Abstract

The synthesis of poly(ethylene terephthalate) (PET) involves the polycondensation of bis(2-hydroxy-ethyl) terephthalate (BHET). This reaction is usually catalysed by species containing antimony (Sb), such as antimony (III) oxide (Sb_2O_3). Besides also being a product of the polycondensation reaction, ethylene glycol (EG) is also added to the system in order to dissolve Sb_2O_3 and form what is believed to be the catalytically active species, antimony (III) glycolate ($Sb(Gly)_2$). In spite of this, EG is believed to also inhibit the catalytic activity of Sb_2O_3 by further reacting with $Sb(Gly)_2$ to form antimony (V) glycolate ($Sb(Gly)_3$), which is a stable species whose formation causes the loss of Sb available in solution to act as a catalyst. This inhibitory effect is known to be significant when the concentration of EG in solution ([EG]) is high, but there are no studies in literature which quantify this range of [EG].

The main objective of this thesis was to perform the kinetic study of a synthetic PET (re)polymerisation system involving purified BHET and EG as starting materials, and Sb_2O_3 as catalyst. By varying the concentration of Sb ([Sb]), the initial amount of EG fed to the reactor (EG_0), the temperature and the precursor of Sb, it was desired to see how these parameters affected the rate of reaction.

It was observed that the rate of reaction was directly proportional to the temperature and [Sb]. However, no clear conclusions could be drawn from the effect of EG_0 and the form precursor of Sb on the rate of reaction. In order to ascertain whether EG presents an inhibitory effect on the catalytic activity of Sb and the ranges of values of EG_0 above which this effect is significant, it was important to proceed to carry out a modelling work.

The objective of the modelling work was to tune parameters of existing reactor models and to propose a new reactor model capable of well predicting the experimental results for all ranges of experimental conditions. The parameters common to all models were the noncatalytic rate constant (k^{th}), the catalytic rate constant (k^{cat}) and the activation energy (E_a). One model proposed one additional parameter to account for the inhibitory effect by EG, k_{inh},. Another model proposed the additional parameters α, β and γ were tuned.

The simplest model, which did not account for the inhibition of Sb by EG, was able to predict well the experimental results when EG_0 was below 25 wt-%, while the more sophisticated models, which took that into account, were able to also predict well the behaviour of the system when EG_0 was equal or greater than 25 wt-%.

Keywords

PET, antimony, ethylene glycol, kinetic study, catalysis, catalytic inhibition, modelling.

Resumo

A síntese do polietileno tereftalato (PET) envolve a policondensação do tereftalato de bis-hidroxietila (BHET). Esta reação é geralmente catalisada por espécies contendo antimónio (Sb), tais como o trióxido de antimónio (Sb_2O_3). Além de ser um produto da reação de policondensação, o etilenoglicol (EG) é também adicionado ao sistema para dissolver Sb_2O_3 e formar o que se acredita de antimónio (III) ser a espécie cataliticamente ativa, o glicolato ($Sb(Gly)_2$). No entanto, acredita-se que o EG também inibe a atividade catalítica do Sb_2O_3, reagindo subsequentemente com $Sb(Gly)_2$ para formar o glicolato de antimónio (V) ($Sb(Gly)_3$), que é uma espécie estável e cuja formação provoca a perda de Sb disponível para atuar como catalisador. Sabe-se que este efeito de inibição é significativo para concentrações de EG ([EG]) elevadas, mas não há estudos na literatura que quantifiquem esta gama de [EG].

O principal objetivo desta tese foi realizar o estudo cinético de um sistema de (re)polimerização do PET, envolvendo BHET purificado e EG como reagentes, e Sb_2O_3 como catalisador. Fez-se variar a concentração de Sb ([Sb]), a quantidade inicial de EG alimentada ao reator (EG_0), a temperatura e a forma do precursor de Sb, de forma a determinar como estes parâmetros afetavam a velocidade da reação.

Observou-se que a velocidade da reação é diretamente proporcional à temperatura e à [Sb]. Porém, não foi possível tirar conclusões claras sobre o efeito de EG_0 e da forma do precursor de Sb na velocidade da reação. De forma a verificar se o EG apresenta um efeito inibidor sobre a atividade catalítica do Sb e as gamas de valores de EG_0 acima dos quais este efeito é significativo, procedeu-se à realização de um trabalho de modelação.

O objetivo do trabalho de modelação foi o de afinar os parâmetros de modelos reacionais existentes na literatura e propor um novo modelo reacional capaz de prever bem os resultados experimentais em todas as gamas de condições experimentais. Os parâmetros comuns a todos os modelos são a constante de velocidade não-catalítica (k^{th}), a constante de velocidade catalítica (k^{cat}) e a energia de ativação (E_a). Um modelo apresenta um parâmetro adicional para explicar o efeito inibitório por EG, k_{inh}. O modelo proposto nesta tese possui os parâmetros adicionais α, β e γ.

O modelo mais simples, que não contabiliza a inibição do Sb por EG, permite prever bem os resultados experimentais quando EG_0 é menor que 25 wt-%, enquanto os modelos mais sofisticados, que tiveram em conta a inibição, são capazes de prever bem o comportamento do sistema quando o EG_0 é igual ou superior a 25 wt-%.

Palavras-Chave

PET, antimónio, etilenoglicol, estudo cinético, catálise, inibição catalítica, modelação.

Contents

List of figures

List of figures from annex

List of tables

List of Abbreviations

Chemical species

Main

PET – poly(ethylene terephthalate)

rPET – recycled PET

BHET – bis(2-hydroxyethyl) terephthalate

EG – ethylene glycol

PET_2 – PET dimer

PET_3 – PET trimer

PET_4 – PET tetramer

Sb_2O_3 – antimony (III) oxide

$Sb(Ac)_3$ – antimony (III) acetate

$Sb(Gly)_2$ – antimony (III) glycolate

$Sb(Gly)_3$ – antimony (V) glycolate

$Sb(Gly)_x$ – antimony-glycolate complex

DEG – diethylene glycol

DMT – dimethyl terephthalate

TPA – terephthalic acid

THF - tetrehydrofuran

Secondary

MHET – mono-(2-hydroxyethyl) terephthalate

BHET·DEG

TiO_2 – titanium oxide

$Zn(Ac)_2$ – zinc acetate

$Pb(Ac)_2$ – lead (II) acetate

$Mn(Ac)_2$ – manganese (II) acetate

PTO – potassium tetraoxalate

$SnO(But)_2$ – dibutyltin oxide

PVC – polyvinyl chloride

EVA – ethylene vinyl acetate

PE – polyethylene

PBT – polybutylene terephthalate

PTFE – polytetrafluoroethylene

ETFE – ethylene tetrafluoroethylene

C_2H_7NO – ethanolamine

H_2O – water

CH_3OH - methanol

Functional groups

COOH – carboxyl

COOR – ester

OH – hydroxyl

CO – carbonyl

Composition

$BHET_0$ – initial wt-% of BHET inside reactor

EG_0 – initial wt-% of EG inside reactor

MS1% – 1 wt-% mother solution of Sb_2O_3 in EG

[Sb] – Sb concentration

$[Sb_2O_3]$ – Sb_2O_3 concentration

[OH] – OH concentration

$[Q_q]$ – concentration of reactant q

$[Q_q]_{eq}$ – concentration of reactant q at equilibrium

$[P_p]$ – concentration of product p

$[P_p]_{eq}$ – concentration of product p at equilibrium

Analytical techniques

SEC – size-exclusion chromatography

HPLC – high-performance liquid chromatography

UV – ultraviolet

RI – refractive index

Kinetics

r – rate of reaction

k – rate constant

E_a – activation energy

k^{th} – noncatalytic rate constant

k_{ref}^{th} – noncatalytic rate constant at T_{ref}

k^{cat} – catalytic rate constant

k_{ref}^{cat} – catalytic rate constant at T_{ref}

k_{inh} – inhibition constant

k^{app} – apparent rate constant

Thermodynamics

K – reaction quotient

K_{eq} – equilibrium constant

$\Delta_r G$ – Gibbs free energy

$\Delta_r H°$ – enthalpy change of reaction

$\Delta_f H°$ - enthalpy change of formation

Experimental part

T_{target} – target temperature

$\Delta t_{correction}$ – correction time

$Conv_{BHET}$ – % of BHET conversion

v_{PET_2} – % of PET_2 formation

Modelling

AVS – AthenaVisual Studio

$\mathcal{FM}$ – activity formalism

α, β, γ – additional parameters defined in the proposed formalism

T_{ref} – reference temperature

SD – standard deviation

CI – confidence interval

R^2 – coefficient of determination

Others

P_n – polymerisation degree

E_s – esterification degree

MW – molecular weight

v – stoichiometric coefficient

V_R – reactor volume

θ – residence time

Subscripts

q - reactant

p – product

i – component

j – reaction

z – set of experimental results

Random

φ – random variable

α – random parameter of model

1 Introduction

1.1 PET data

Poly(ethylene terephthalate), more commonly known as PET, is a thermoplastic polyester with excellent chemical and physical properties for many implementations. Its most important properties include excellent chemical resistance, excellent wear resistance, wide economic availability, easy process ability, extremely low moisture absorption, low flavour adsorption, very good colour stability and good resistance to thermal aging [1].

For this reason, PET is amongst the most widely used polymers worldwide today, with its global demand having reached 27 million metric tons in 2020 and, by 2030, it is predicted to increase to 42 million metric tons [2]. The main applications of PET include textiles, bottling, food packaging, thermoplastic resins and PET sheets. In 2019, the distribution of PET packaging consumption worldwide by end-use sector is given by Figure 1-1.

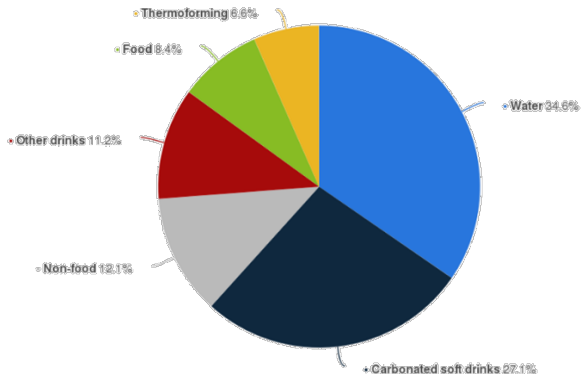

Figure 1-1: Distribution of PET packaging consumption worldwide in 2019, by end-use sector [3].

Bottled water accounted for most of the global PET consumption and, in 2016, 485 billion PET bottles were produced, whose number is also expected to increase to 583 billion in 2021 [4]. PET and plastic waste is a highlighting issue for humans and for the environment [5]. Plastic products' main application are short-term living and disposable packaging material, which become waste after single-use. From 1950 to 2015, it is estimated that 6.3 billion tons of plastic waste was generated, around which 9% was recycled, 12% was incinerated and 79% was accumulated in landfills or in nature [5]. Hence, a big amount of plastic waste has been accumulated and is accumulated in the environment, as each year, around 1 million metric tons of plastic end up in landfill or in the ocean [5].

In Europe, over 1,9 million tons of PET bottles were collected for recycling in 2017, comprising a recycling rate of 58.2% [6]. However, new bottles placed on the EU market contain an average of just 17% of recycled-PET (rPET) [6]. By 2025, PET beverage bottles will have a mandatory rPET content of 25%, which will increase to 30% in 2030 [6].

1.2 PET industrial synthesis

A condensation polymer, PET resins are usually produced commercially by the reaction between ethylene glycol (EG) and either dimethyl terephthalate (DMT) or terephthalic acid (TPA) [7]. Both synthesis processes will be described in Sections 1.2.1 and 1.2.2. The industrial synthesis can take place both batchwise and continuously, and the reactors used for these processes is also suitable for the production of other thermoplastic polyesters [8].

It should be noted that both routes account for a number of secondary reactions which occur predominantly during the polycondensation step [8]. These can alter the stoichiometric ratio and terminate the polycondensation reaction at undesired times or give undesirable properties to the PET formed [8]. The most frequent secondary reaction is the formation of diethylene glycol, DEG, which can be incorporated in the polymer and damage its dyeing behaviour and lower its thermal and UV stability [8]. Other secondary reactions include the dehydration of EG to form acetaldehyde, ester pyrolysis to give carboxyl groups, COOH, and alkenes [8].

1.2.1 DMT route

This synthesis route involves the reaction between EG, which is produced commercially by the reaction between ethylene oxide and H_2O, and DMT, which is produced through the direct esterification of TPA with methanol [8]. It is a two-stage process, involving a transesterification and a polycondensation step, and separate vessels are often used to melt the starting compounds and for the transesterification and polycondensation reactions [8].

The main advantages of this synthesis route as compared to that which uses TPA to produce PET, which will be described forward, are the following:

- No need for expensive, high corrosion resistant reaction vessels, due to no environmentally aggressive chemicals being used [8];
- DMT is easy to purify compared to TPA [8].

1.2.1.1 Transesterification step

DMT is first melted at 150-160ºC in a stirred tank heated with steam, carrier oil, or electricity in an inert atmosphere made up usually of N_2 [8]. The molten DMT is then transferred to a transesterification reactor, where it reacts with EG at 150-200ºC [8]. The reaction takes place at 1 atm, in a N_2-rich atmosphere, and, initially, the lower temperatures in the range mentioned are preferred in order to minimise the sublimation of DMT. This temperature is then raised as the reaction proceeds [8].

As shown in Figure 1-2, this reaction produces bis(2-hydroxyethyl) terephthalate (BHET), which is the comonomer of PET and reactant in the polycondensation step, and methanol, which is continuously distilled off from the reaction mixture [8]. The use of catalysts is indispensable to achieve a reasonable rate of transesterification at moderate temperatures [8]. The most widely used catalysts in this step are

weakly basic compounds, such as zinc acetate, $Zn(Ac)_2$, lead (II) acetate, $Pb(Ac)_2$, and manganese (II) acetate, $Mn(Ac)_2$ [1].

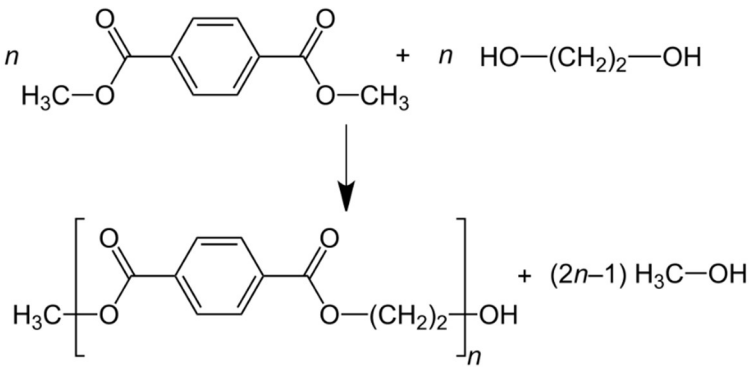

Figure 1-2: Transesterification step in DMT route [9].

1.2.1.2 Polycondensation step

The transesterification product is added, still in liquid state, to the polycondensation reactor, which can be heated to above 300ºC and must be equipped with a very efficient stirrer [8]. Initially, the excess EG from the transesterification step is distilled off at 1 atm by gradually increasing the temperature to *ca.* 250ºC. In the polycondensation step, BHET polymerises to form PET and EG (by-product).

For the polycondensation step to take place, a reduction in pressure and a further increase in temperature are necessary [8]. In order to obtain PET with sufficiently high molecular masses, the reaction must take place at a vacuum of *ca.* (1-5)x10^{-4} atm and at temperatures of *ca.* 270-280ºC [8]. Additionally, to have a high rate of polycondensation, the EG produced must be constantly distilled off from the reaction mixture [8]. The reaction is stopped when a defined melt viscosity, which is intrinsically related to the molecular mass of PET, is reached [8].

The main catalysts used in this step are those based on antimony (Sb), such as antimony (III) oxide, Sb_2O_3, and antimony (III) acetate, $Sb(Ac)_3$ [1].

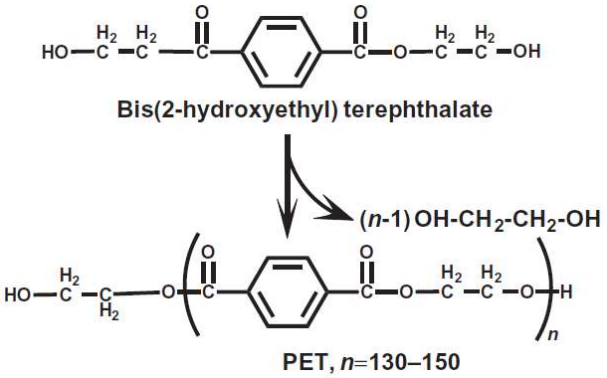

Figure 1-3: Polycondensation step of DMT route [1].

1.2.2 TPA route

Unlike the DMT route, the TPA route proceeds in a single reactor. However, it too is a two-stage process, which involves the direct esterification between TPA and EG (in excess) to produce BHET and H_2O as a by-product, which is constantly distilled off, followed by the polycondensation of BHET to produce PET, as shown in Figure 1-4 [8]. The reactor is placed under high temperatures of *ca.* 220-260ºC and at high pressures of *ca.* 2.7-5.5 atm, in order to give high rates of reaction [8]. Due to the sparing solubility of TPA in EG, the reaction medium is heterogeneous, although the use of high temperatures and excess of EG are attempts to overcome this sparing solubility [8].

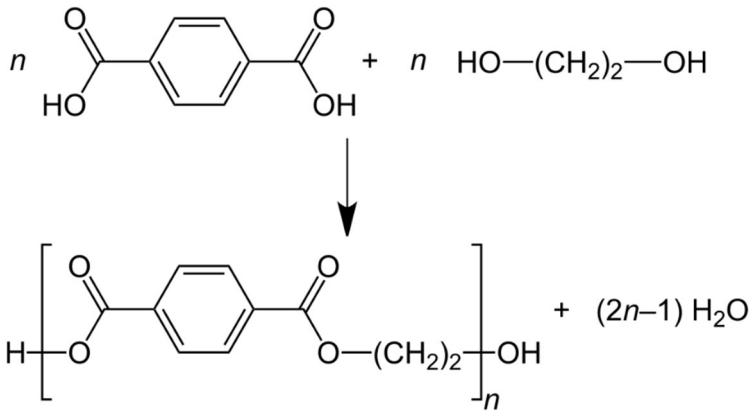

Figure 1-4: Synthesis of PET using TPA and EG as reactants [9].

As in the polycondensation step of the DMT route, Sb-based catalysts, such as Sb_2O_3 and $Sb(Ac)_3$ are the main catalysts used for this reaction [8]. In new industrial plants for the production of PET, this route is preferred over the DMT route, as the former shows many advantages over the latter, such as:

- Higher rate of reaction [8];
- Lower molecular mass of TPA (166.13 g/mol) compared to DMT (194.19 g/mol) [8];
- PET of higher molecular masses obtained [8];
- H_2O is easier to distil off from the reaction mixture than EG [8].

1.3 Contamination of PET

Due to the non-existence of living organisms capable of naturally degrading its large molecules, PET is a non-degradable plastic in normal conditions [10]. Furthermore, their extensive use and slow rate of decomposition means that the waste management of PET products is considerably hard and creates environmental pollution problems [11] [10]. For this reason, the recycling of post-consumer PET began in order to address the environmental pressure to improve waste management [10].

In order to achieve successful PET recycling and to be suited for high-value applications, the flakes of rPET should meet certain minimum requirements, which are summarized in Table 1-1 [11].

Table 1-1: Minimum requirements for post-consumer PET flakes to be processed [10].

Properties	Values
Intrinsic viscosity	> 0.7 dlg^{-1}

Melting temperature	> 240°C
Water content	< 0.02 wt-%
Flake size	0.4 mm < suitable value < 8 mm
Dye content	< 10 ppm
Yellow index	< 20
Metal content	< 3 ppm
Polyvinyl chloride content	< 50 ppm
Polyolefin content	< 10 ppm

The contamination of post-consumer PET is one of the biggest problems affecting its recyclability and the major cause of deterioration of its physical and chemical properties during reprocessing. More specifically, due to fibre breakage and aesthetic problems, contamination cannot be allowed for fibre or bottle applications. Minimization of contamination leads to better quality of rPET. The most common sources of contamination will be described below.

1.3.1 Acids

Acidic compounds catalyse the chain-scission reactions of the ester linkages of PET [10]. These typical contaminants include polyvinyl chloride (PVC), glue, dirt, ethylene vinyl acetate (EVA) and paper. The most harmful acids are acetic acid (produced by EVA from the cap liners), rosin acid and abietic acid (produced by adhesives from the label) and hydrochloric acid (produced by PVC flakes from PVC bottles) [10].

1.3.2 Water

The presence of moisture can induce molecular weight reduction by hydrolysis [10]. For this reason, moisture contamination should be below 0.02 wt-% [10]. Most of this water content comes from the flake washing process, but it can be significantly reduced by commercial dryers, operated at 150°C for 4 hours [11].

1.3.3 Labels and adhesives

PET labels are normally made with ultrathin polyethylene (PE) films, which can be difficult to separate if used extensively. The adhesives used to glue the labels to the PET can also cause problems in recycling, because some of the glue may be retained in the PET and be incorporated into the recycled resin [11].

1.3.4 Colouring contaminants

Dyes form coloured bottles and printed ink labels can cause undesirable colours during reprocessing [10]. Additionally, the latter can also discolour the PET flakes in the washing process [10]. The reduction of these colouring contaminants is achieved by improving sorting and washing techniques in bottle recycling [10].

1.3.5 Acetaldehyde

Being a major by-product of PET degradation reactions, acetaldehyde is present in both PET and post-consumer PET [10]. The migration of acetaldehyde into food products from PET containers is a major

concern, as it can affect taste and aroma [11]. Due to its high volatility, so their production can me minimised by processing under vacuum or by drying [10]. Additionally, stabilisers such as 4-aminobenzoic acid, diphenylamine and 4,5-dihydroxybenzoic acid can be added to PET in order to minimize the amount of acetaldehyde produced [10].

1.3.6 Metals

The manufacturing of PET employs the usage of various metals which act as catalysts [11]. Furthermore, metals are also present in dyes, which are used in coloured PET. These metals remain as residues trapped inside the PET throughout its life [11]. These metals promote the transesterification, polycondensation and direct esterification reactions, and lead to the chemical heterogeneity of the recycled PET, which affects its melt rheological behaviour [11].

These main metals, their respective common concentrations inside the PET and their origin are shown in Table 1-2. One interesting aspect of these metals is that, as they remain trapped in the PET, they can be reused as catalysts in the chemical recycling of PET. This is especially true for Sb, whose compounds are the most widely used catalysts in the polycondensation and direct esterification reactions for the synthesis of PET. As shown in Table 1-2, the concentration of Sb, [Sb], trapped in PET is usually in the range of *ca.* 220-240 ppm and, depending on the reaction media and conditions, it can become catalytically active in the chemical recycling of PET. This Sb is referred to as inherited Sb.

Table 1-2: Various metal ions in recycled PET, their usual concentrations and origins [11].

Metal	Concentration (ppm)	Origin
Sb	220-240	Polycondensation catalyst
Co	50-100	Transesterification catalyst
Mn	20-60	Transesterification catalyst
Ti	0-80	Polycondensation catalyst
Fe	0-6	Washing

1.4 PET recycling

PET recycling is the best method for waste management, as it provides opportunities for reducing the dependency on fossil fuels as a raw material in PET production (thus minimizing carbon dioxide (CO_2) emissions) and decrease the load on landfill space [12]. Thus, recycled PET has a prospective to substitute virgin PET from refined fossil fuels. On top of that, the energy required to produce recycled polymers is less than that to produce virgin polymers from fossil fuels [12].

Existing PET recycling methods can be summarized in 4 categories:

- Primary recycling: in-plant recycling of uncontaminated, clean industrial scrap PET [13].
- Secondary (mechanical) recycling: sorting, washing, drying and melt processing [13].
- Tertiary (chemical) recycling: depolymerization reaction, decontamination and re-polycondensation process (depolymerization, purification and then repolymerization) [13].

1.4.1 Mechanical recycling of PET

Mechanical recycling of post-consumer PET normally consists of the removal of contaminants by sorting and washing, drying and melt-processing [11]. Mechanical recycling is more practiced than chemical recycling, but leads to the degradation of its properties, while high-quality end-products can be achieved using chemical recycling method, allowing them to repolymerize to virgin grade plastic. The main advantage of the mechanical recycling is its simplicity, environmentally friendliness and low investment requirement [10]. Its main disadvantage, however, is the reduction of its melting point during processing, due to a decrease in its viscosity [10].

Mechanical recycling is widely used to recycle PET bottles and, due to the quality loss caused by thermal and hydrolytic degradation, the rPET obtained is normally applied in lower value uses, such as textiles [10]. However, it is of great challenge to recycle the PET fibres through mechanical recycling due to the complexity of textile products and presence of many additives, such as pigments, dyes and dispersants [10]. Around 70% of the rPET is used for fibre applications and most of them are either downcycled into lower value products or end up in landfills or incinerators [10]. This open-loop recycling is unsustainable and more reasonable solutions should be explored for the recycling of post-consumer PET materials, especially for PET fibres and for complex and heterogeneous waste streams [10].

1.4.1.1 Removal of contaminants

This first step consists of several processes in which post-consumer PET bottles are sorted, ground and washed [10]. The sorting process is basically separating PET bottles from PVC, PE and other plastic containers [10]. The sorting of PET bottles is an important step, because high levels of contamination by other materials causes great deterioration of post-consumer PET during processing [10]. After sorting, the post-consumer PET is ground into flakes, which can be easily washed and, subsequentially, reprocessed [10].

1.4.1.2 Drying

Minimizing the moisture content of post-consumer PET flakes reduces its degradation by hydrolysis and leads to higher melt strength in the rPET [10]. Typically, no more than 50 ppm water is allowed to be present in the PET flakes and this is normally achieved by using desiccated dryers operating at 170°C for 6 h before feeding to the extruder [10].

1.4.1.3 Melt-processing

Post-consumer flakes can be processed in a normal extrusion system to give useful granules [10]. However, due to the contaminants present in post-consumer PET, the granules produced by extrusion at 280°C in the presence of those contaminants tend to have a low molecular weight, due to degradation reactions [10].

1.4.2 Chemical recycling of PET and glycolysis

Chemical recycling is a novel method for PET recycling which consists in the degradation of PET waste into monomers (and oligomers), which are first purified and can be subsequently used for the production of high-quality rPET via repolymerization [14]. This is the most promising way to achieve the closed-loop recycling for all PET waste and is carried out by solvolysis, which is a chemical reaction in which the solvent, present in a huge excess to its stoichiometric amount, is one of the reagents used to bring about the depolymerisation at high temperatures and in the presence of catalysts.

Depending on the solvent used, the processes have different names and produce different monomers, which can be polymerised again to produce rPET. These are summarized in Table 1-3.

Table 1-3: Solvent and monomer produced for each solvolysis process.

Process	Solvent	Monomer produced
Hydrolysis	H_2O	TPA
Mathanolysis	CH_3OH	DMT
Aminolysis	C_2H_7NO	bis(2-hydroxyethylene)terephthalamides
Ammonolysis	NH_3	p-xylylenediamine or 1,4-bis(aminoethyl)cyclohexane
Glycolysis	EG	BHET

Glycolysis is the most popular method to depolymerise waste of PET and a promising way to achieve the closed-loop recycling for PET in a commercial scale, due to its mild conditions and weak volatility of EG [5] [14]. In this process, the post-consumer PET is depolymerized into BHET, which can be polymerized again to produce rPET. Chemically, glycolysis involves the molecular cleavage of PET by glycols (usually EG), in the presence of transesterification catalysts, and the breakage of ester linkages and their replacement with hydroxyl (OH) terminals [13].

The main products obtained from the glycolysis reaction are BHET and short-chain oligomers, all of which can be further processed to manufacture other products, such as polyurethane foams, hydrophobic dye stuffs, unsaturated resins and acrylic coatings. The BHET obtained from glycolysis can be mixed with fresh BHET and be used to produce PET. Glycolysis involves the following steps [13]:

1. Initiation: carbonyl carbon of ester group of the polymer is attacked by the free electron pair present on EG.
2. OH ethyl group of EG bonds with carbonyl carbon of PET, which breaks long polymer chain into short oligomers with subsequent formation of BHET.

Factors like reaction time, temperature, pressure and ratio of PET to solvent affect the rate of glycolysis, but, in order to have a decent rate of reaction at moderate temperatures and pressures, it is important to use of a catalyst in the glycolysis of PET. Metal based transesterification catalysts are commonly for this matter [13]. The mechanism of PET glycolysis, both uncatalysed and catalysed, is given in Figure 1-5. As mentioned previously, there are always trapped metals in solid PET, mainly Sb, at low concentrations. Depending on the reaction media and conditions, these can act as catalysts in the glycolysis as well.

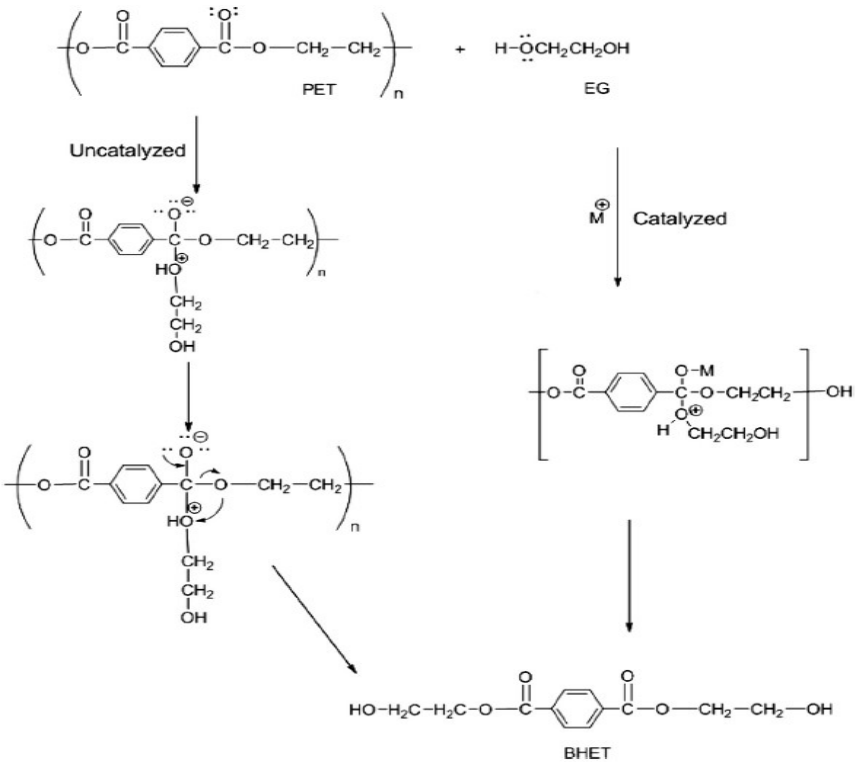

Figure 1-5: Mechanism of PET glycolysis, to give BHET, both uncatalysed and catalysed by a metal compound [13].

1.5 Thesis objective

The objective of the current thesis is to perform the kinetic study of a synthetic PET (re)polymerisation system involving BHET (obtained from the glycolysis of PET) and EG as starting materials, and Sb_2O_3 as catalyst. The BHET had been previously purified, as to not contain inherited substances, such as inherited catalyst metals and dyes, which may have been present in PET.

As will be described in Section 1.6, despite being essential for activating Sb_2O_3 allowing it to become catalytically active, EG is also thought to inhibit the catalytic activity of Sb_2O_3, and this inhibition is believed to become greater as [EG] increases. This hypothesis is based on experimental studies on PET polymerisation which showed that Sb-based catalysts have low activity in at high [OH], whose main source is EG, which contains two OH end-groups [15]. Despite this observation, the range of [EG] above which this inhibition effect is significant is not known, and this is due to the lack of studies performed on this topic. Furthermore, the system studied in the current thesis is different than that of industrial PET polycondensation involving the same reactants. As will be explained in Section 1.7, in the current system, only a short-chain oligomers were formed, while the reaction in industrial polycondensation allows for the formation of long-chain oligomers and the PET polymer. Therefore, it was also desirable to know if the catalytic activity of Sb_2O_3, was inhibited by EG in the current system.

The scheme of the system studied in the current work is shown in Figure 1-6, where PET_2, PET_3 and PET_4 refer to the dimer, trimer and tetramer of PET, respectively, whose chemical structures are shown in Annex A.

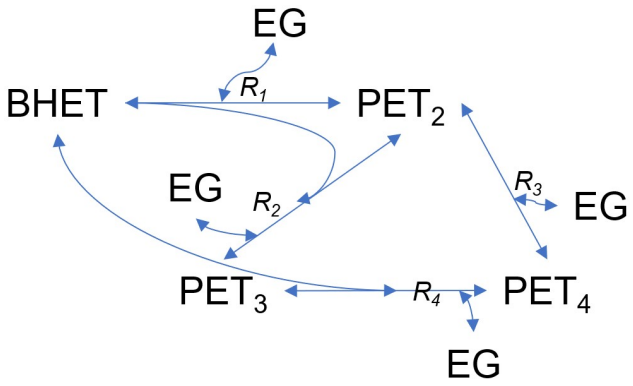

Figure 1-6: Scheme of reactions studied in the current system.

By varying the amount of Sb_2O_3 fed to the reactor, which will, in turn, affect the concentration of Sb in the reaction medium, it would be possible to investigate the effectiveness of Sb_2O_3 as a catalyst in the polycondensation of BHET. At the same time, by varying the initial reactant composition of the reactor, *i.e.*, the initial ratio of BHET to EG, $BHET_0$:EG_0, and the concentration of Sb_2O_3, it would be possible to observe the effect of EG on the catalytic activity of Sb_2O_3 and the value of EG_0 above which it would be possible to observe, if at all, its inhibition effect on the catalytic activity of Sb.

In the current work, the concentration of Sb, [Sb], was considered instead of the concentration of Sb_2O_3, [Sb_2O_3]. This is because, in most experiments, Sb_2O_3 was not added directly to the reactor, but rather first dissolved in EG to make a mother solution, which was then added to the reactor, as will be described in Section 2.3.2. Given that the chemical form which Sb_2O_3 took when dissolved in EG is unknown, in order to standardise the quantification of the concentration, [Sb] was considered.

By varying $BHET_0$:EG_0, it would also be possible to observe how the initial concentration of reactant, $BHET_0$, affects the rate of reaction. The polymerisation of PET is a reversible process and, as such, there will be an equilibrium composition. The driving force of the reaction will be proportional to the magnitude of the difference between $BHET_0$:EG_0 and BHET:EG at equilibrium, $BHET_{eq}$:EG_{eq}.

The choice of the synthetic system with purified BHET was done as to guarantee that all Sb came from the added catalyst. If inherited Sb had been present in the BHET at an unknown concentration, it would not be possible to know [Sb] precisely, which would greatly affect the interpretation and the reliability of the modelling work performed. Additionally, other inherited substances, such as dyes and acetaldehyde, which could affect the progress and outcome of the reaction should not be present, emphasising the importance of having pure BHET. However, due to its hygroscopic nature, some H_2O was present and, even it dried, H_2O was still absorbed from the air when BHET was transferred to the reactor, whose quantify was not accounted for, as will be described in Section 2.1.

Side products, such as DEG, could also be formed in secondary reactions. As mentioned in Section 1.2, these too could have a negative impact on the reaction and their formation is greatly conditioned by the choice of catalyst. Sb-based catalysts show a high selectivity towards the main reaction, so the formation of these was expected to be low.

The experimental work was proceeded by a modelling work, in which a reactor model was defined in attempt to replicate the behaviour of the real reactor. In the reactor model, various formalisms which accounted for the catalytic activity of Sb were defined. Some of the formalisms were found in literature, while others were proposed based on experimental results. These different formalisms had different parameters, which needed to be fitted based on the experimental data and took different factors into account. Some took into account only the catalytic activity of Sb, whilst others also took into account the inhibition effect of EG.

1.6 State-of-the-art

Although widely used as a polycondensation catalyst in the manufacture of PET, as described by Stevenson *et al.*, the catalytic effect of Sb_2O_3 on the transesterification reaction is not fully understood [16]. For this reason, Yamada studied its effect on the reaction between TPA and EG. Contrary to how it is performed in industry, the direct esterification and the polycondensation steps were performed in two separate tank reactors at 1 atm. However, EG and TPA were fed in the esterification reactor in a molar ratio EG:TPA of 2:1 (excess of EG), and both reactors were operated at 250ºC [16].

Yamada concluded that Sb_2O_3 accelerates the transesterification reaction between TPA and EG but has a minor effect on secondary reactions [16]. Intrinsic viscosity is a measure of how much the solute contributes to the total viscosity of a solution. It is not a direct measure of a polymer's molecular weight, but a measure of the size of a polymer coil in solution, which is directly proportional to its molecular weight. For this reason, intrinsic viscosity can be indirectly used as a measurement of molecular weight and polymerisation degree, P_n.

By measuring the intrinsic viscosity of the reaction products of both reactors, it was shown that, as [Sb] increases, both the transesterification degree, E_s, and P_n increase, which indicates that Sb_2O_3 catalyses both the transesterification and the polycondensation reactions [16]. It was also shown that, during polycondensation, Sb_2O_3 has a suppressing effect in the formation of diethylene glycol (DEG) because, as [Sb] increases, the content of DEG decreased [16]. This can be explained by the fact that, as [Sb] increases, although the kinetics of DEG formation also increases, the concentration of OH groups decreases, and the effect of this decrease preponderates [16].

Chen *et al.* studied the formation of DEG as a side-product in the synthesis of PET using Sb_2O_3 as a catalyst [17]. By analysing the product of the reaction through gas chromatography, it was shown that Sb_2O_3 has a minor effect on the depolymerisation reaction but, contrary to Yamada's findings, this catalyst also increases the rate of formation of DEG, both in the transesterification and in the polycondensation steps, although the effect on the former is greater. Additionally, it was also shown that this increase is linearly proportional to [Sb] and inversely proportional to P_n, which means that the rate of formation of DEG is highest at the beginning of the polycondensation and decreases with time [17]. The formation of DEG should be kept as low as possible due to the problems caused by its presence in PET, as mentioned in Section 1.2, and also due to competitive catalytic inhibition, as both the main reaction and the formation of DEG are catalysed by Sb_2O_3.

It should be noted that the system studied by Yamada is different to that studied by Chen *et al.*. The former studied a system comprised of TPA and EG as the sole reactants, and had the esterification and polycondensation steps performed in different reactors, both operated at 250ºC, 1 atm and with a mean residence time of the reaction mixture, θ, of five hours [16]. The latter, on the other hand, studied a system comprised of a three-component reactant mixture of PET oligomers, TPA and EG [17]. Additionally, the reaction was performed over a shorter time period (less than three hours) and in a single reactor, whose temperature and pressure were changed throughout the reaction [17]. This difference in the reaction conditions could be the cause of the different conclusions drawn about the effect of [Sb] in the rate of formation of DEG by both works.

The work performed by Yamada and Chen *et al.* show that Sb_2O_3 is indeed a good catalyst, not only for the polycondensation reaction, as it is mostly used in industry, but also for the transesterification reaction. This catalyst shows a high catalytic activity and selectivity towards PET, thus reducing the amount of undesired reactions, such as the depolymerisation of PET and the formation of secondary products, such as DEG and aldehydes, which have a negative impact on the polymeric properties. In the work performed in the current thesis, the reaction which was studied was the Sb_2O_3-catalysed polycondensation reaction of a synthetic system comprising of BHET and EG in a batch reactor. This corresponds to a different system and operating conditions to those studied in the cited works, but it still involves the polycondensation of BHET and the use of Sb_2O_3. For this reason, it can be expected that Sb_2O_3 will be a suited choice of catalyst.

Shah *et al.* investigated the influence of the nature and concentration of various metal catalysts on the rate of polycondensation of BHET to PET [18]. The reaction was carried out at *ca.* 290°C in a 250 mL tube reactor, in which BHET was introduced in a DMT vapour bath and, once the BHET had melted, the catalyst was added in a nitrogen (N_2) atmosphere [18]. The polymer was extruded into cold water to stop the reaction and a capillary viscometer (with phenol-tetrachloroethane as solvent) was then used to determine its intrinsic viscosity, in order to determine each catalyst's activity [18]. A higher value for the intrinsic viscosity corresponded to higher catalytic activity, because catalytic activity is directly proportional to P_n [18].

By analysing the viscosity of the PET formed, it was shown that the most effective transesterification catalysts, such as $Pb(Ac)_2$, $Zn(Ac)_2$ and $Mn(Ac)_2$ (as mentioned previously) are the least effective polycondensation catalysts [18]. Similarly, it was shown that the most effective polycondensation catalysts, such as potassium tetraoxalate (PTO), dibutyltin oxide ($SnO(But)_2$) and Sb_2O_3 were the least effective transesterification catalysts [18]. This finding was in accordance with the choice of catalysts used in industry in the DMT route for the production of PET, as described in Section 1.2.

When looking at the three polycondensation catalysts, it was possible to observe that PTO showed the greatest catalytic activity, while Sb_2O_3 showed the smallest. An interesting discovery was that, although increasing the catalyst concentration also increased the rate of reaction, this was only true up to a certain catalyst concentration, after which the rate of reaction began to decrease, meaning that each catalyst has an optimum concentration, corresponding to a maximum of catalytic activity, as can be seen in

Figure 1-7 [18]. This optimum concentration is different for each catalyst, but it is in the range of *ca.* (1.5-2.5)x10^{-4} mol/mol_{BHET}.

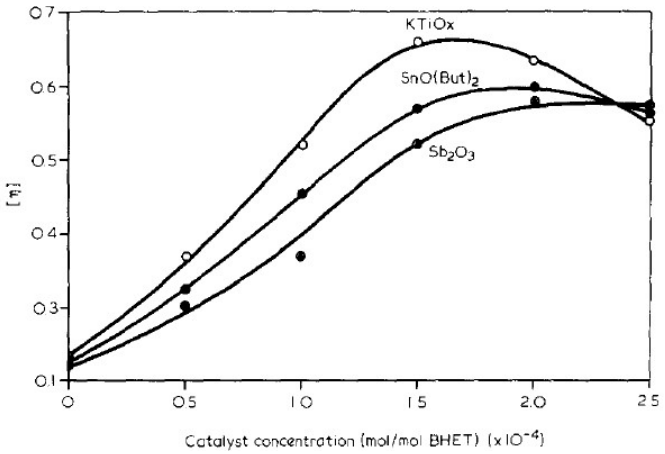

Figure 1-7: Effect of catalyst concentration on the polymerisation of BHET [18].

Figure 1-7 also shows that this decrease was inversely proportional to the catalyst's activity, meaning that PTO showed the biggest decrease and Sb_2O_3 showed the smallest [18]. This is explained by the fact that the increase in the catalyst concentration enhanced both the polymerisation and the depolymerisation reactions [18]. When the concentration of catalyst increased above the optimum, there starts to be competition between the catalytic sites responsible for the polymerisation reaction and the catalytic sites responsible for the depolymerisation reaction [18]. As polymerisation proceeds, the concentration of BHET (and its OH end-groups) falls, meaning that less of it binds to the metal catalyst [18]. This frees up space for the oxygen in the ester linkages of the PET to bind to the catalytic sites and undergo the degradation reaction [18].

The work by Shah *et al.* is important because it shows that, despite Sb_2O_3 showing a lower catalytic activity compared to Ti- and Sn-based catalysts, it shows a greater range of applicability, *i.e.*, it still shows a high catalytic activity at high [Sb]. This makes Sb_2O_3 an interest subject of study for the current thesis, both because it is usually inherited in rPET, and also because it is desired to observe the effect of Sb_2O_3 as a catalyst at a wide range of concentrations.

El-Toufaili *et al.* carefully studied the mechanism of the Sb_2O_3-catalysed polycondensation reaction of BHET [15]. It is generally accepted that polycondensation proceeds by the nucleophilic attack of the oxygen from the OH group (O–OH) at the end of the chain of one oligomeric molecule on the carbon from the carbonyl group (C–CO) from the end of the chain of another oligomeric molecule. However, neither the catalytic mechanism nor the catalytically active species are fully known. El-Toufaili *et al.* proposed that the catalyst either activates the attacking O–OH by forming a metal alkoxide, or it activates the attacked C–CO by complexation with the oxygen from the carbonyl group (O–CO) or from the ester group (O–COOR) [15].

After investigation in IR spectroscopy, thermal analysis, kinetic studies and literature review, the following mechanism for the Sb_2O_3-catalysed polycondensation was proposed by El-Toufaili *et al.*, which starts with the reaction between Sb_2O_3 with EG in the reaction medium to produce antimony (III)

glycolate, $Sb(Gly)_2$, as shown in Figure 1-8. $Sb(Gly)_2$ is thought to be the catalytically active species. This is an example of homogeneous catalysis.

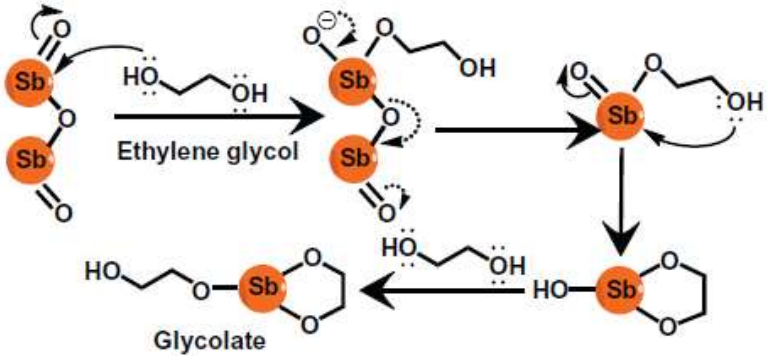

Figure 1-8: Activation of S_2O_3 by EG to form $Sb(Gly)_2$, the catalytically active species [1].

As will be explained later, the polymerisation of PET is not a single-, but rather a multi-step process, which means that the growth of the polymer chain happens in several steps involving the reaction between two oligomers, always intermediated by catalytically active species. Firstly, $Sb(Gly)_2$ reacts with an oligomeric species to produce an organometallic intermediate, with the release of EG as a by-product, as shown in Figure 1-9.

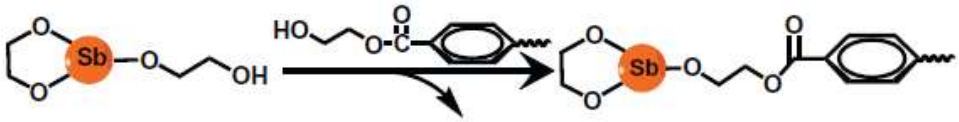

Figure 1-9: Reaction of $Sb(Gly)_2$ with an oligomeric molecule to form an organometallic intermediate [1].

Secondly, the organometallic intermediate reacts with another oligomeric species to give a new oligomeric species with the combined chain length of both previous oligomers, with the release of another molecule of EG as a by-product and the regeneration of $Sb(Gly)_2$, as shown in Figure 1-10. This step includes the formation of a transition state in which both oligomeric molecules are ligands to the Sb atom, and the intramolecular rearrangement of the complex's coordination sphere is driven by the reestablishment of the chelate structure of $Sb(Gly)_2$, which is very stable.

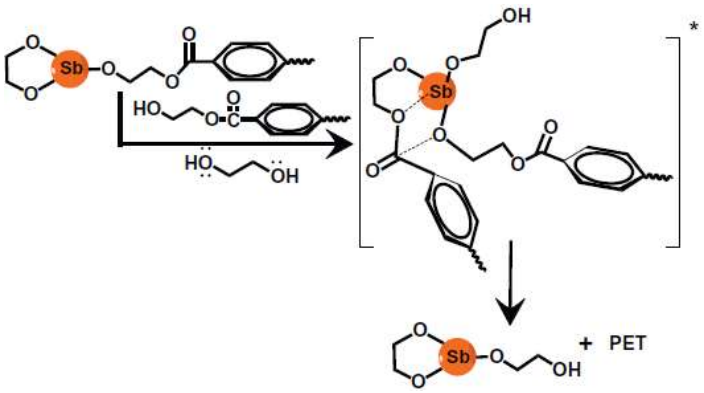

Figure 1-10: Reaction between organometallic intermediate and a second oligomeric molecule to form the final long chain oligomeric molecule and regenerate $Sb(Gly)_2$ [1].

The work performed by El-Toufaili *et al.* is of utmost importance to the current thesis because, not only it proposed a mechanism for the polycondensation of PET catalysed by Sb_2O_3, but it also found that Sb

is not catalytically active in OH-rich media, due to the formation of stable Sb-glycolate complexes, $Sb(Gly)_x$, which have also been studied by Maerov. The clarification of the mechanism for Sb catalysis and the reason behind its low activity when [OH] is high is useful for future catalyst development [15].

Maerov performed an experimental study involving the polymerisation of BHET to determine the effect of the number, chelation and type of ligand on the degree of polymerisation and rate of reaction [19]. Despite EG being necessary to activate Sb_2O_3 to form $Sb(Gly)_2$, it has been proposed that EG could further react with $Sb(Gly)_2$ to give antimony (V) glycolate, $Sb(Gly)_3$, whose neutral structure is shown in Figure 1-11.

This neutral form of $Sb(Gly)_3$ is thought to be unstable, and Maerov proposed that it is quickly converted into its ionic form, which is shown in Figure 1-12, by deprotonation [19]. This ionic form is highly stable isolatable, which means that Sb remains trapped as $Sb(Gly)_3$, thus decreasing the amount of Sb available to combine with O–OH and O–COOR end-groups from oligomers and reducing its catalytic activity [19]. For this reason, EG is said to also inhibit the catalytic activity of Sb-containing species, like Sb_2O_3, and this phenomenon is specially significant at high [EG]. This is the reason why Sb-containing species are not effective catalysts for transesterification, given the high [EG] in the reaction medium. However, they are much more effective polycondensation catalysts, due to lower [EG].

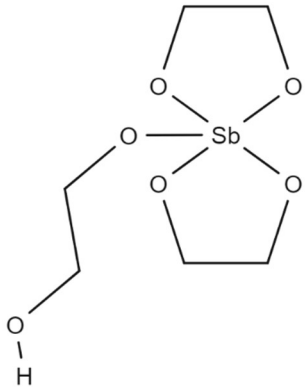

Figure 1-11: Molecular structure of the neutral form of $Sb(Gly)_3$.

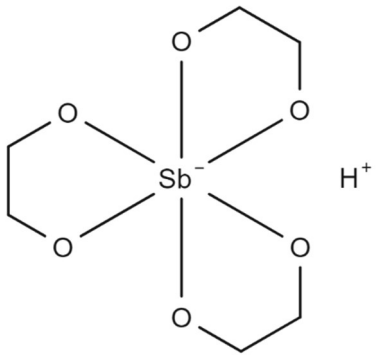

Figure 1-12: Molecular structure of the ionic form of $Sb(Gly)_3$.

Maerov showed that EG plays a critical role in the catalytic activity of Sb_2O_3, given that it is necessary to produce $Sb(Gly)_2$, which is proposed to be the catalytically active species, but EG may also further react with $Sb(Gly)_2$ to form $Sb(Gly)_3$, thus decreasing the catalytic activity of Sb, given the high stability and low catalytic activity of $Sb(Gly)_3$. This formation of this species might become specially significant at high [EG], but, despite this proposal, neither Maerov nor any other study available in literature studied this phenomenon carefully or specified the range of [EG] above which the inhibition of the catalytic activity of Sb by EG starts to become significant and hinder the rate of reaction. El-Toufaili *et al.* also proposed that the formation of unreactive products between Sb and BHET may also decrease the catalytic activity of Sb [15].

Furthermore, the formation of other OH-containing species, such as DEG, may also influence the reaction, as they too could react with Sb_2O_3 to form catalytically active or unactive species, which may cause the reaction to proceed through a different mechanism. It was shown by both Yamada and Chen

et al. that Sb-based catalysts are highly selective towards PET and have little effect on promoting secondary reactions, such as the production of DEG, so they are a good choice of catalyst to study the effect of EG on the catalytic activity of Sb_2O_3. For this end, work still remains to be done.

Both Yamada and Duh *et al.* proposed that the rate constant of the polycondensation of PET, k, is directly proportional to [Sb], as shown in Equation I [16] [20]. This proposition is very simple, because it assumes that the reaction is of first order with respect to Sb and it does not take in to account the inhibition effect of EG on the catalytic activity of Sb, which was described previously. Furthermore, Duh *et al.* specified that the correlation shown in Equation I is only valid for [Sb] ≤ 100 ppm, above which the catalytic activity of Sb appeared to reach a plateau, whose value is different for each temperature in the range 210-230ºC, which was the range studied by Duh *et al*. [20]. It should be noted that Duh *et al.* studied solid-state polycondensation, and at a higher range of temperatures than the one studied in the current work, which will be described in Section 2.3.3, but this correlation was still applied to the current system, given it was also proposed by Yamada, which studied the direct esterification of PET in liquid phase, despite not specifying the range of [Sb] to which it was applicable.

$$k \propto [Sb] \qquad \text{I}$$

Hovenkamp studied the kinetics of the catalysed esterification reaction in a glycoldibenzoate–glycol–glycolmonobenzoate model system [21]. This three-component model system was chosen because it allowed for the utilization of lower reaction temperatures (below 200ºC) and because it did not produce a mixture of oligomers, whose reactivities could affect the interpretation of results [21]. Furthermore, the equilibrium constant of the esterification reaction for the model system was shown to be almost equal to that for the polymeric system [21]. Like Yamada and Duh *et al.*, Hovenkamp proposed that k is directly proportional to [Sb], but also inversely proportional to the concentration of OH, [OH], as shown in Equation II.

$$k \propto \frac{[Sb]}{[OH]} \qquad \text{II}$$

It is known that [OH] is related to [EG], because it is the OH groups in EG which bind to Sb. Equation II takes into account the inhibition effect of EG, and Hovenkamp defined its applicability in the range [Sb]/[OH] of *ca.* 0-2 mol/kg, at temperatures in the range of 170-197ºC. The temperature range is similar to the one studied in the current work (described in Section 2.3.3), but it offers a rather unclear range of applicability, not to mention that Equation II was derived based on studies performed on a synthetic esterification system.

In order to address this problem, a final proposition was found in literature [22]. Like Yamada, Duh *et al.* and Hovenkamp, it suggested that the rate of reaction was directly proportional to [Sb]. However, it also suggested that the rate of reaction decreased with an increase in [EG], according to a Langmuir rate expression, as shown in Equation III [22]. In this expression, k is shown to be inversely proportional to 1+φ[EG], where φ is a constant.

$$k \propto \frac{[Sb]}{1 + \varphi \times [EG]} \quad \text{III}$$

As will be shown in Section 0, the correlations given by Equations I and III will be adapted to construct formalisms for the catalytic activity of Sb. Despite not being derived based on the exact same system studied in the current thesis, these correlations can still be studied to see how well they fit to the experimental results of the current thesis, given that both [Sb] and [EG] are factors to be studied.

1.7 Reaction Kinetics

Reaction kinetics involves the experimental study of the rates of chemical reactions, *i.e.*, the rate at which reactants, *q*, are turned into products, *p*, and the factors which influence the rates, and the explanation of the rates based on the reaction mechanisms of chemical processes [23]. Kinetic studies are generally conducted to determine the most appropriate reaction rate model that is fundamentally derived from mechanistic reaction pathways in order to capture the experimental reactant reaction rate and the product formation rate with the best fit [24].

For any chemical reaction, the mechanism refers to the sequence of elementary steps (usually), *i.e.*, single-step reactions with a single transition state and no intermediates, by which the overall chemical change occurs. If the chemical conversion of reactants into products involves more than one elementary step, then the chemical structures that exist after each elementary step preceding the final product formation are known as intermediates.

PET is a condensation polymer, which means that it is formed through step-growth polymerisation. This is a type of multi-step polymerisation that relies on the presence of reactive functional groups in two different molecules (usually at the end of the backbone) to react with each other and produce intermediary molecules with increasingly longer polymer chains, with the formation of a small molecule as a by-product [25].

In the case of PET polymerisation, an COOR function from one molecule reacts with an OH function from another molecule, the intermediate molecules formed are called oligomers, *i.e.*, low molecular weight polymers comprising a small number of repeating units whose physical properties are significantly dependent on the length of the chain, and the small molecule formed as by-product is EG.

Each of these intermediate reactions in PET polymerisation is reversible. The general form of an equilibrium reaction is shown by Equation IV [26], where *q* and Q refer to the reactants species and *p* and P refer to the products species, and ν_q and ν_p refer to the stoichiometric coefficients of reactants and products, respectively.

$$\sum_q \nu_q \times Q_q \leftrightarrow \sum_p \nu_p \times P_p \quad \text{IV}$$

A reversible reaction can proceed in either direction, depending on the temperature and on the concentrations of reactants, *q*, and products, *p*, relative to the corresponding equilibrium concentrations. In order to understand in which direction the reaction is likely to proceed, it is necessary to define a term

called the reaction quotient, K, which measures the relative amounts of products, *p*, and reactants, *q*, present during a reaction at a particular point in time. For a reversible reaction with the form given by Equation V, K is given by Equation V, where $[Q_q]$ and $[P_p]$ are the concentrations of reactants, *q*, and products, *p*, respectively, at a particular point in time.

$$K = \frac{\prod_p [P_p]^{\nu_p}}{\prod_q [Q_q]^{\nu_q}} \quad \text{V}$$

As the reaction proceeds, $[Q_q]$ and $[P_p]$ also change and approach their equilibrium values, $[Q_q]_{eq}$ and $[P_p]_{eq}$. For this reason, the value of K will also change and approach its equilibrium value, K_{eq}, also known as the equilibrium constant, whose formula is given by Equation VI. For this reason, in order to calculate K_{eq} from experimental results, it is necessary to carry out reactions until equilibrium, *i.e.*, the state in which $[Q_q]$ and $[P_p]$ have no net change over time.

$$K_{eq} = \frac{\prod_p [P_p]_{eq}^{\nu_p}}{\prod_q [Q_q]_{eq}^{\nu_q}} \quad \text{VI}$$

The bigger the difference between these two quantities, the bigger is the driving force for the reaction. This is due to the Gibbs free energy, $\Delta_r G$, of the system, whose form for a reversible reaction is given by Equation VII [26]. It is possible to observe that, the bigger the difference between K and K_{eq}, the bigger the magnitude of $\Delta_r G$ and the bigger the driving force of the reaction. When K equals K_{eq}, $\Delta_r G$ becomes equal to zero and there is no more driving force for the reaction, meaning that [Q] and [P] no longer change, assuming that only the polymerisation reaction takes place (as was considered in the model).

$$\Delta_r G = R \times T \times \ln\left(\frac{K}{K_{eq}}\right) \quad \text{VII}$$

According to Le Chatelier's principle, a disturbance in [Q] and [P] and temperature will cause the dynamic equilibrium of the system to shift to counteract the change and re-establish equilibrium. When the disturbance is in [Q] and [P], the value of K_{eq} is not altered, and the shift in the equilibrium of the system will be such as to re-establish the values of $[Q_q]_{eq}$ and $[P_p]_{eq}$ given by K_{eq}. However, when the disturbance is in the temperature, the values of K_{eq}, $[Q_q]_{eq}$ and $[P_p]_{eq}$ will also change, and the shift in the equilibrium will be such as to establish a new equilibrium. The relationship between the temperature of the system and K_{eq} is given by the Van't Hoff equation (Equation VIII).

$$\frac{d[\ln(K_{eq})]}{dT} = \frac{\Delta_r H^\circ}{R \times T^2} \quad \text{VIII}$$

By integrating the Van't Hoff equation between two temperature values, T_1 and T_2, it is possible to arrive at the form of the Van't Hoff equation given by Equation IX, which allows for the calculation of K_{eq} at temperature T_2 by knowing its value at temperature T_1 and by knowing $\Delta_r H°$. The enthalpy of reaction, $\Delta_r H°$, for polymerisation reactions are close to zero, *i.e.*, they are athermal, as will be explained forward. For this reason, it is possible to conclude that K_{eq} will not be affected by temperature.

$$\ln\frac{K_{eq_2}}{K_{eq_1}} = -\frac{\Delta_r H°}{R} \times \left(\frac{1}{T_2} - \frac{1}{T_1}\right) \quad \text{IX}$$

In the case of PET polymerisation, two BHET (monomer) molecules begin by reacting with each other to form one dimer (PET_2) molecule and one EG molecule (by-product). The remaining BHET molecules can now either react with one another again in the same reaction, or react with the newly formed PET_2 molecule, to produce a trimer (PET_3) molecule (with EG as a by-product). As more PET_2 and PET_3 are produced, the number of possible reactions and species formed also increases, giving way for the formation of the tetramer (PET_4) and longer chain oligomers, thus growing the polymer chain. The general form of the chemical equation of the intermediary reaction between two PET oligomers with *m* and *n* repeating units, respectively, is given by Equation X.

$$PET_m + PET_n \leftrightarrow PET_{m+n} + EG \quad \text{X}$$

The reactions in this multi-step process are all reversible reactions. In industry, the production of PET from BHET is usually carried out in a series out continuous reactors and at temperatures above 200°C, which means that small molecules, like EG, which has a boiling point of 197°C, are vaporised and evacuated from the system through scrubbers. In the present work, however, the polymerization reaction is carried out in a single batch reactor and at temperatures below the boiling point of EG, meaning that there is no way to remove the EG produced.

For this reason, due to Le Chatelier's principle, the equilibrium of intermediate reactions given by Equation X are greatly shifted to the side of reactants and the polymer chain does not grow significantly. For this reason, only the reaction up to PET_4 was considered, as the formation of longer-chain oligomers was considered negligible. This allowed for the kinetic study of the formation of small-chain oligomers. Furthermore, the analytical techniques used, which will be described in Section 2.3.5, allowed only for the quantification up to PET_4. Table 1-1 shows, for each reversible reaction, *j*, the corresponding rate equation, r_j, kinetic rate constant (for the forward reaction), $k_{j\rightarrow}$, and the equilibrium constant, K_{eq_j}.

Table 1-4: Reactions considered to be taking place in the current system.

	Chemical equation	Rate equation
R_1	$2 \times BHET \overset{k_{1\rightarrow}}{\leftrightarrow} PET_2 + EG$	$r_1 = k_{1\rightarrow}\left([BHET]^2 - \frac{[PET_2][EG]}{K_{eq_1}}\right)$
R_2	$BHET + PET_2 \overset{k_{2\rightarrow}}{\leftrightarrow} PET_3 + EG$	$r_2 = k_{2\rightarrow}\left([BHET][PET_2] - \frac{[PET_3][EG]}{K_{eq_2}}\right)$
R_3	$BHET + PET_3 \overset{k_{3\rightarrow}}{\leftrightarrow} PET_4 + EG$	$r_3 = k_{3\rightarrow}\left([BHET][PET_3] - \frac{[PET_4][EG]}{K_{eq_3}}\right)$
R_4	$2 \times PET_2 \overset{k_{4\rightarrow}}{\leftrightarrow} PET_4 + EG$	$r_4 = k_{4\rightarrow}\left([PET_2]^2 - \frac{[PET_4][EG]}{K_{eq_4}}\right)$

As is visible in Table 1-4, the rate constant for the reverse reaction, $k_{\leftarrow j}$, was not explicated, but rather written in terms of $k_{j\rightarrow}$ and K_{eq_j}, by the formula shown in Equation XI. Given that $k_{\leftarrow j}$ and $k_{j\rightarrow}$ are always related by K_{eq_j}, it was not necessary to discretise $k_{\leftarrow j}$.

$$K_{eq_j} = \frac{k_{j\rightarrow}}{k_{\leftarrow j}} \qquad \text{XI}$$

For any of these reactions to proceed, the breakage of two C–O bonds and the formation of two new C–O bonds must occur, as is shown in Figure 1-13, which depicts the reaction R_2 from Table 1-4. These bonds do not have the exact same bond formation enthalpies, $\Delta_f H°$, given they are present in different molecules. However, given that two bonds of the same type were broken and other two bonds of the same type were formed, it can be assumed that $\Delta_r H°$ is approximately zero, thus meaning that K_{eq} does not vary significantly with temperature in this case.

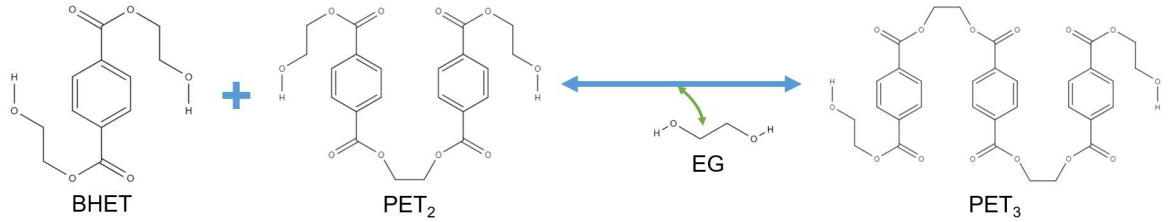

Figure 1-13: Reversible reaction between BHET and PET_2 to form PET_3.

2 Methodology

2.1 Materials

Only three different species were added to the reactor: EG, Sb_2O_3 and BHET.

The EG used had a purity of over 99.5% and was from the supplier Carlo Erba. It is a transparent solvent and was used as a solvent, both in the preparation of the mother solution of catalyst, which will be discussed forward, and in the reaction medium as a reagent. In both cases, EG has a critical role in dissolving Sb_2O_3 and making it catalytically active in the medium.

The Sb_2O_3 used had a purity of over 99% and was from the supplier Sigma-Aldrich. It is a white powder and was the source of catalyst which was used. The Sb_2O_3 was either dissolved in EG to prepare a mother solution (homogeneous precursor of Sb), or it was added directly in powder form to the reactor (heterogeneous precursor).

The BHET used was obtained from the glycolysis of PET, realised at IFPEN. This BHET was purified and dried before being used in the current work, in order to guarantee that it did not contain significant quantities of inherited substances, *eg.* Sb or Ti, which act as catalysts in the system. This would make the real catalyst concentration inside the system unknown and greatly affect the reliability of the analyses and of the modelling work. For this reason, it was important to use a pure source of BHET, so that all other species present in the reactor came from their addition to the reactor, and were not inherited.

2.2 Apparatus

2.2.1 Dry bath heater

Dry bath heaters are extremely versatile laboratory equipment designed to maintain constant temperatures. They can accommodate a variety of vessels and be used in a variety of different applications, such as sample preparation, enzyme preservation and enzyme-substrate reactions, and electrophoresis gel degeneration. They have advanced internal temperature sensing probes for temperature accuracy and control (with a PID circuit), which allow the user to offset the temperature to the desired value and to adjust any temperature deviations.

As a good temperature control is desired for the present work, a dry bath heater was chosen in order to accommodate the reactors and bring them to the desired temperatures for the reaction and the dissolution. One of the available dry bath heaters can accommodate two autoclave reactors and six glass reactors, as will be discussed forward.

2.2.2 Autoclave

This type of reactor was used in order to prepare the mother solution of Sb_2O_3 in EG. The boiling point of EG at atmospheric pressure is 197°C and, due to the temperature of the reactor being raised until 200°C, it was expected that, despite strong agitation, some of the EG would evaporate. Given that the dissolution takes place in a batch reactor, this evaporation of EG in the closed reactor would lead to a build-up of pressure inside the closed recipient, which could lead to the danger of container rupture if a glass reactor was used. Due to this safety reason, the autoclave reactor was used.

2.2.3 Glass reactors

The repolymerisation reactions were carried out inside 250 mL glass bottles. These bottles are made up of borosilicate glass, which have exceptionally low thermal expansion coefficients, making them more resistant to thermal shock than the normal glass. These also have high thermal capacity, good chemical and thermal resistance, smooth and easy-to-clean surfaces, and are highly inert. Their uniform wall thickness distribution also allows for uniform heating.

2.2.4 Stirring

Stirring allows for the equilibration of temperature and concentration differences in the reaction medium, allowing for the homogenisation of mixable liquids and solid particles dispersed in liquids. Furthermore, the stirring of liquids speeds up the dissolution process and increases the speed of chemical reactions.

The preparation of the mother solution of Sb_2O_3 in EG involves dissolution, which is a physico-chemical process by which the solute (Sb_2O_3) is incorporated in a solvent (EG) to form a homogenous mixture (solution). The oligomerisation of BHET is a chemical process that leads to the formation of low molecular weight PET oligomers. Both processes are carried out at high temperatures and with stirring in order to speed up the rates of reaction and dissolution.

There are two types of stirring: magnetic and the mechanical stirring. In the present work, magnetic stirring was chosen. For magnetic stirring to occur, it is necessary to have a stationary electromagnet that creates a rotating magnetic field, which then causes the magnetic bar immersed in a liquid solution to rotate. The dry bath heater had this electromagnet coupled inside it.

The cleaning and sterilisation of stirring bars is achieved much more easily than that of mechanical stirrers, due to their small sizes and simple geometry. They are also much cheaper and easier to apply in closed systems, such as bath reactors, than mechanical stirrers. Their drawback is their efficiency for low volumes (<4 L) and low viscosities only. None of these are relevant to the present work, because small volumes (~10 mL for the reaction and ~100 mL for dissolution) and low-viscosity liquids are used.

2.2.5 Temperature measurement

Thermocouples were used in order to measure the temperature of the contents inside the autoclave and glass reactors. Thermocouples are electrical devices made up of two wires of dissimilar electrically conducting materials (generally metals or metal alloys) that are joined at one end and left open at the other end. Due to their different heat capacities, when the junction is heated, a temperature difference between the two metals is generated, which in turns produces an electromotive force, as a result of the Seebeck effect.

The range of temperatures used in the present work are well within the range of temperatures allowed for the thermocouples:

- 20ºC – 200ºC for the preparation of the mother solution.
- 20ºC – 190ºC for the reactors.

For the preparation of the mother solution, as two autoclaves were used (each to prepare 100 mL of solution), one thermocouple was assigned to each autoclave.

2.3 Methodology

2.3.1 Catalyst studied

The catalyst studied was Sb, which is the most widely used polycondensation catalyst in PET production. The source of Sb used was Sb_2O_3, which is a white fine powder and one of its most commonly used sources, along with $Sb(Ac)_3$. Furthermore, Sb_2O_3 is commonly dissolved in EG to make a liquid solution, in which case Sb would be present as a homogenous catalyst.

Sb_2O_3 has limited solubility in EG and, for this reason, a solution of only 1 wt-% of Sb_2O_3 in EG ([Sb] = 8353 ppm) was prepared, which was similar to the one prepared by El-Toufaili *et al.* ([Sb] = 8500 ppm) [15]. Sb_2O_3 can also be used directly in powder form (heterogenous precursor). Given that the Sb in heterogenous form would have to dissolve in the reaction medium in order to act as a catalyst, a reduced activity or a conversion delay might appear on tests carried out with Sb_2O_3 powder instead of pre-dissolved Sb.

2.3.2 Preparation of the mother solution

A mother solution of 1 wt-% of Sb_2O_3 in EG (MS1%) was envisaged. By considering the atomic and molar masses of Sb and Sb_2O_3 and Sb's atomic subscript in Sb_2O_3, this would be equivalent to a solution of 8353 ppm of Sb in EG. In order to prepare enough solution for the entire duration of the internship and to suffice the amount of catalyst needed for every test intended, two solutions of about 100 g (100 mL) each were prepared. For this reason, two autoclaves were used.

First, after cleaning them with acetone, the mass of each autoclave was measured. Secondly, about 100 g of EG were added into each autoclave. Before Sb_2O_3 was added, however, the EG in both autoclaves was degassed by sparging with argon (Ar). The sparging was done by dipping a thin metal syringe in the EG, turning on the flow of gas and stirring gently for around 2 minutes.

Figure 2-1: Needle used to degas the reactors with Ar.

According to Henry's law, the amount of each dissolved gas in a liquid is proportional to its partial pressure above the liquid [35]. Sparging introduces a gas that has little or no partial pressure and increases the area of the gas-liquid interface, which encourages some of the dissolved gases to diffuse into the sparging gas before the sparging gas escapes from the liquid [35]. The most widely used gas for sparging is air. However, to remove O_2, a chemically inert gas such as N_2, Ar or He is used.

After degassing, Sb_2O_3 was added to the EG using a spatula. After measuring the mass of EG added, a magnetic agitator was added inside each autoclave. After putting a band around the top of the autoclave, it was firmly closed and degassed again, to remove any traces of O_2 that might have entered during the addition of Sb_2O_3. This time, degassing was done with the autoclaves closed, by placing the plastic capsule of the needle around the metal tube of the autoclave.

The information of the masses of each autoclave and the masses of EG and Sb_2O_3 added to each autoclave, as well as the final mass concentration of Sb, [Sb], in the solution inside each autoclave is shown in Table 2-1.

Table 2-1: Masses of autoclaves, masses of EG and Sb_2O_3 added to each autoclave, and resulting [Sb].

	Mass autoclave (g)	Mass EG (g)		Mass Sb_2O_3 (g)	Sb (ppm)
		Before degassing	After degassing		
1	3886.62	100.14	100.13	1.03	8.50×10^3
2	3879.61	100.00	99.98	1.00	8.27×10^3

The thermocouples were placed inside the autoclaves, which were put inside the dry bath heaters and surrounded by wool. The dry bath heater was turned on to a target temperature of 200°C and a rotational speed of the magnetic agitator of 1500 rpm. Due to the thick walls of the autoclaves, it took several hours for the contents inside them to reach the target temperature of 200°C. the dry bath heater was switched off at the end of the day, and the solutions were left to cool down during the night.

The following morning, the autoclaves were opened to check the appearance of the solutions and if there was any undissolved Sb_2O_3 present. After realising that there was still some undissolved, the autoclaves were once again closed, degassed and put inside the dry bath heater, which was turned on in the same conditions as the day before.

The dry bath heater was again turned off at the end of the day, and the appearance of the solutions was observed the next morning. There were no visible traces of undissolved Sb_2O_3 in the solution in either autoclave, so the solutions were transferred to two glass flasks, and stored for future use.

2.3.3 Operating conditions

The effect of the rotational speed on the rate of reaction was not a variable which was desired to be investigated and, for this reason, all experiments were conducted at a rotational speed of 1000 rpm. Given that it was desired to carry out a kinetic study of the repolymerisation reaction of PET, the main variables whose effect on the reaction rate was desired to be studied were the initial BHET:EG (reactants) ratio, the concentration of Sb (catalyst) and the form of the catalyst (MS1% or Sb_2O_3 powder).

Due to there being the constraint of the time required for analysis, it was necessary to plan in advance all the compositions of the samples to be studied, in order to have a range of compositions as wide as possible. The initial BHET:EG ratio, $BHET_0$:EG_0, was varied from 1:0 to 3:2 (wt). This range of ratios were selected as to always have a higher amount of BHET than of EG, to guarantee a fast enough rate of reaction.

Given that Sb is dissolved in EG in MS1%, if MS1% had been used as the only source of Sb, [Sb] would always be limited by the mass percentage of EG and, subsequentially, by $BHET_0$:EG_0. It is possible to further dilute MS1% by adding pure EG, as was done to prepare the solutions given by the orange points, but it is not possible to further concentrate it. For this reason, it is not possible, for a given $BHET_0$:EG_0, to obtain a [Sb] above the one given by the grey points.

In order to overcome this constraint, Sb_2O_3 powder can be used as the source of Sb in alternative to MS1%. Despite being a very fine powder, thus harder to manipulate than MS1%, [Sb] and $BHET_0$:EG_0 can be changed independently, thus allowing the preparation of compositions with low mass percentages of EG, but high [Sb], which are shown by the yellow points. The use of Sb_2O_3 powder would also allow for the investigation of the differences in activity between the homogenous and the heterogeneous catalyst.

It is also worth mentioning the blue and green point, which refer to the samples prepared without adding any catalyst. It was important to have these points because, despite having a low rate, the uncatalyzed reaction still takes place.

The reference temperature, T_{ref}, was chosen to be 180°C, and most experiments were carried out at this temperature. This temperature was selected because, as mentioned previously, the boiling point of EG at atmospheric pressure is 197°C and, because the reactions were all carried out in glass reactors, as will be mentioned later, it is important to prevent the formation of vapour, which would build up the

pressure inside the reactor, as this vapour is not allowed to leave from the batch reactor, and possible cause the reactor to rupture.

On the other hand, it was not desired to carry out the reaction at a low temperature either, because that would have negative implications on the rate of reaction. In industry and in other works found in literature, the reaction is usually carried out at above 200°C. For this reason, a compromise T_{ref} of 180°C was chosen, as it would also be possible to carry out the reaction at slightly higher or lower temperatures, without the formation of EG vapor, and without decreasing too much the rate of reaction.

Since it was also desired to obtain an estimate of E_a for the polymerisation of PET, it was necessary to carry out the reaction at more than one temperature. The Arrhenius equation is a simple, but remarkably accurate formula for the temperature dependence of the chemical reaction rate constant. By knowing the values of k at two different temperatures, T_1 and T_2, it is possible to write the Arrhenius equation as shown by Equation XII, which allows for the determination of E_a.

$$k_{T_2} = k_{T_1} \times \exp\left(-\frac{E_a}{R}\left[\frac{1}{T_2} - \frac{1}{T_1}\right]\right) \qquad \text{XII}$$

With the intention of estimating E_a, compositions of EG_0 and [Sb] equal to 12.5 wt-% and 1000 ppm were also performed at 170ºC and 190ºC. Given that this was not the main objective of the current work, only this composition was performed at three different temperatures, because, as will be described forward, the number of samples that could be sent to analysis was limited. For this reason, it was more important to focus on performing experiments over a wide range of compositions than on performing experiments at other temperatures just to estimate E_a.

2.3.4 Experimental procedure

First, the glass reactors (and their plastic caps) and the magnetic agitators were cleaned with acetone, in order to remove organic residues, and were weighted separately in a precision balance. One magnetic agitator was put inside each glass reactor.

After measuring the masses of the empty reactors (with the magnetic agitators), the desired masses of reactants were carefully added into each reactor. The BHET was the first reactant to be added to the reactor, as it was always the one added in greater quantity and because it was a solid. The addition of BHET was aided with a plastic funnel and a metal spatula.

Next, the pure EG and MS1% or Sb_2O_3 powder were added. For the pure EG and MS1%, both were carefully added with Pasteur pipettes. In the case of Sb_2O_3 powder, it was necessary to use an analytical balance and a weighing boat, as only very small masses of the powder were needed (the precision balance did not have enough precision), and it was a difficult material to handle. The powder was carefully transferred to a weighing boat (with known mass) with a spatula (both cleaned with acetone) and the desired masses were carefully measured before being transferred to the reactors.

After being filled with the samples, the reactors were closed with the red cap. The total mass of reactants inside each reactor was always equal to 10 g.

A dry bath heater has six positions, which means that, at one time, it can accommodate six different reactors. Due to the small masses (and volumes) of reactants inside each reactor, if samples were taken at different times, the volume of liquid left inside the reactor would be very small. Furthermore, due to the high temperature of the reactors, it would be difficult to take samples, because it would involve opening the lid of each reactor at the required time, and taking samples (with a glass pipette, for example), which would need to be quickly transferred to another recipient, otherwise it would solidify inside the pipette. Furthermore, when opening the reactor, there would be losses due to evaporation and the temperature would be affected, which would have a negative impact on the rate of reaction.

For these reasons, sampling of the reactors was not done. Instead of preparing six reactors with six different compositions, every two reactors were prepared with the same composition, giving three pairs of reactors with three different compositions in the dry bath heater at a given run. Each reactor in the pair was removed and had the reaction stopped at a different time, in order to be to analysis and obtain information about the composition and, subsequently, the rate of reaction. By following this procedure, it would be possible to obtain information about the progress of the reaction of each composition at three different times:

- t_0: initial composition.
- t_1: time at which the first reactor in the pair was removed from the dry bath heater.
- t_2: time at which the second reactor in the pair was removed from the dry bath heater.

The composition at t_0 was known with high certainty, given it was the initial composition of every reactor before the reaction. The compositions at t_1 and t_2 were obtained by sending them to analysis. These times were measured using a stopwatch, as will be described later. The choice of t_1 and t_2 was done individually for each pair of compositions. In general, the lower [Sb] and the higher EG_0, the lower the rate of reaction is expected to be and, for this reason, the bigger the values of t_1 and t_2 chosen. This is because a higher rate of reaction will lead to a higher conversion of reactants for a given time. Usually, t_1 was half of t_2. Furthermore, the temperature of the reaction was also considered for the choice of t_1 and t_2. For a given composition, the values of t_1 and t_2 were higher for smaller temperatures and lower for higher temperatures, because the rate of reaction is directly proportional to the temperature. The reactions were stopped by placing the glass reactor inside a cold-water bath, in order to quickly decrease its temperature and solidify the contents inside it. Solids have very low reactivities, so it could be considered that the reactivity of the solidified product was null. The solidified product was then broken with the help of a metal spatula and transferred to a small glass flask to be sent to analysis. As mentioned previously, two thermocouples were available for temperature measurement, which means that the temperature of the contents inside two reactors could be measure simultaneously. In order to measure these temperatures, a hole was punched on two of the plastic caps in order to allow the passage of the thermocouple. The two caps with the hole were always put on the two reactors which would stay on the dry bath heater for the longest, in order to be able to measure the temperature for as long as possible. Readings of the temperature of both thermocouples was taken at regular intervals (temperature profile), in order to keep track of the temperature inside the reactor, check for abnormalities or discrepancies, and to make necessary adjustments if needed.

2.3.5 Analytical techniques

2.3.5.1 Size-exclusion chromatography

Size-exclusion chromatography (SEC) is considered the most common, efficient and fastest method that provides information about a polymer's molecular weight (MW) average and its MW distribution [36]. SEC separates molecules in a sample according to their hydrodynamic volumes (volume of a polymer coil when in solution) instead of their MW [36].

In this technique, a stationary phase (gel consisting of spherical beads containing pores of a specific size distribution) is placed in a column, and the mobile phase (organic solvent) that contains the sample solution is injected into the stationary phase. The molecules that are larger than the pore volume will be eluted first (in the column's void volume) due to their inability to penetrate the pores, whereas the smaller molecules will take a longer time to be eluted because they can penetrate the pores. Molar masses are determined either from a calibration or using molar mass sensitive detectors.

For the optimisation of the resolution in SEC, *i.e.*, of the accuracy of the molecular-weight distribution measurements, it is necessary to either increase the pore volume in the column or increase the column efficiency [37]. The former is limited by nature, because a high pore volume leads to limited pressure stability [37]. Consequently, improvement of column efficiency must be achieved by reducing the particle diameter [37]. Small particle diameters of *ca.* 3 µm are advantageous because they allow for the operation at usual liquid chromatographic velocities of *ca.* 3 mm/s, thus achieving short analysis times [37]. The problems associated with the use of such small particles are negligible in the size-exclusion mode, thus allowing for the use of larger column diameters [37].

Another important requirement of SEC is that the molecules should not react with or have any affinity with the resin material of the column. The separation must be governed by size alone [38]. Additionally, the resin must be properly packed in order to ensure that the molecules are able to enter the pores or pass between the beads as predicted [38]. Overpacking a column can block the pores, whilst underpacking a column can reduce the chances of small molecules being trapped in the pores, both of which can lead to poor resolution and broad elution peaks [38].

The internal diameter of the column affects the flow rate and injection volume. There are two common internal diameters for columns used in SEC: 4.6 and 7.8 mm [39]. Since the separation relies on diffusion into and out of the pores of the stationary phase, the greatest separation comes from having larger column sizes [39]. Using a slow flow rate allows the molecules sufficient time to diffuse [39]. The normal flow rates for SEC columns with internal diameters of 4.6 mm and 7.8 mm are 0.35 mL/min and 1.0 mL/min, respectively [39].

Once the analyte leaves the column, it is directed towards a detector, which is then able to recognise the separated components of the initial mixture. There are many types of detectors, *e.g.*, refractive index (RI) and ultraviolet (UV) detectors.

RI detectors are among the simplest types of detectors, and their operating principle consists in measuring the change in refractive index [40]. They contain a chamber which is split into two cells: one

reference cell, which is filled only with mobile phase, and a sample cell, to which the effluent of the column constantly flows through [40]. An illustration is shown in Figure 2-2. A beam of light is directed at the chamber and, due to the difference in refractive index between the components of both cells, bending of the incident light occurs [40]. By measuring this bending, the presence of components can be observed [40].

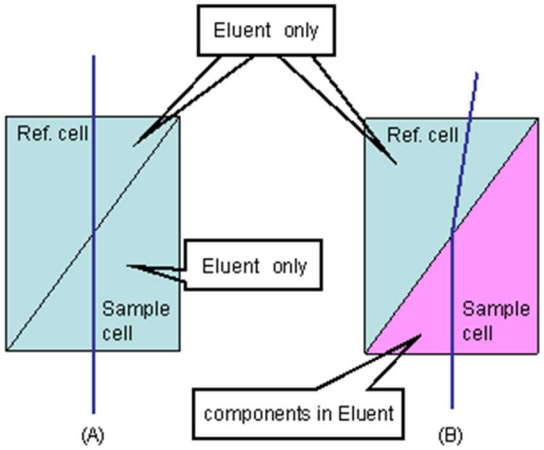

Figure 2-2: Ri detector [40].

UV detectors are absorbance detectors. They are extremely sensitive, easy to operate and provide good stability, being the most widely used type of detectors in SEC and HPLC. These detectors consist of a colourless glass cell, through which the effluent is passed (flow cell) [40]. UV light is irradiated on this flow cell and the sample absorbs part of it [40]. The analyte can be identified by measuring its absorption of UV light at different wavelengths [40]. Given that the UV absorbance differs depending on the wavelength used, it is important to choose an appropriate wavelength based on the nature of the analyte [40]. A standard UV detector allows user to choose wavelength between 195 to 370 nm [40]. Most commonly used is 254 nm [40].

RI detectors have lower sensitivity compared to UV detectors, but they are suitable for detecting a much broader range of components. This is because a change in reflective index occurs for all analyte, whilst there are many types of compounds which do not absorb UV radiation and cannot be detected via a UV detector. UV detectors also cannot be used when the mobile phase absorbs UV radiation, while RI detectors can.

2.3.5.2 High-performance liquid chromatography

High-performance liquid chromatography (HPLC) is, like SEC, a chromatography technique used for the separation of different components in a mixture. However, unlike SEC, in which components are separated solely based on their relative sizes, the basic principle of HPLC is that it separates a sample into its constituent parts based on the relative affinities of distinct molecules for the mobile phase and the stationary phase used in the separation [41].

Using a high-pressure infusion system, this method pumps mobile phases, such as single solvents with different polarities or mixed solvents and buffers in different proportions, into a chromatographic column

equipped with extremely fine particles and a high-efficiency stationary phase [42]. After the components in the column are separated, they enter the detector to be analysed [42].

Depending on the chemical structure of the analyte, the molecules are retarded while passing through the stationary phase [43]. The specific intermolecular interactions between the molecules of a sample and the packing material define their retention time [43]. Hence, different constituents of a sample are eluted at different times, allowing for the separation of the components in a mixture. A detection unit, *e.g.* UV detector, recognizes the analytes after leaving the column [43].

Similarly to SEC, the choice of flow rate, stationary and mobile phases, particle and pore size, and column dimensions play a key role in the running time, efficiency and resolution of the analysis [44]. Silica-based materials are physically strong and will not shrink or swell, being compatible with a broad range of polar and non-polar solvents, and, therefore, are often a good choice for the stationary phase [44]. Additionally, if an extremely high resolution of analysis is not required, it is possible to speed up the separation by increasing the flow rate or shorting the column length [44].

Smaller particle sizes provide higher separation efficiency and higher chromatographic resolution, while larger particle sizes offer faster flow rates at lower column back-pressure and clog less easily, meaning that they are more tolerant to matrix effects [44]. Typical particle sizes range from *ca.* 3 µm to 20 µm, being 5 µm usually best compromise between efficiency and back-pressure for most non-high throughput applications [44].

In general, packing materials with a smaller pore sizes have higher surface areas and higher capacities than those with larger pore sizes [44]. A larger surface area typically indicates a greater number of pores, and therefore a higher overall capacity [44]. Smaller surface areas equilibrate faster, which is important for gradient elution analyses [44]. If a molecule is larger than the pore, size exclusion effects will be seen and it will be difficult or impossible to retain it [44].

2.3.5.3 Analytical uncertainty

The relative analytical uncertainty, both in SEC and HPLC analysis, is estimated to be ±10%. This is due, not to the chromatographic process, but rather to the dilution of the samples in THF and the UV detector. Given that both SEC and HPLC employed these two steps, the uncertainty in both of these methods can be considered the same.

3 Experimental results

3.1 Effect of [Sb]

In order to observe the effect of [Sb] on the rate of reaction, it was important to plot graphs in which all other parameters ($BHET_0$:EG_0, temperature and catalyst precursor) were kept constant, and only [Sb] was changed. It was one of the easiest parameters to observe the effect because, given that $BHET_0$:EG_0 was kept constant, the driving force for the reaction was the same for every test, and only the catalyst concentration was varying.

Figure 3-1 and Figure 3-2 shows the change in the mass fractions of BHET and PET_2, respectively, for three different tests performed at T = 180°C and with Sb from MS1%, but with varying [Sb]. It is possible to see that, as [Sb] increases, the rate of reaction also increases, given the higher amount of BHET that reacted ($Conv_{BHET}$) and the higher amount of PET_2 which formed (v_{PET_2}) after a given time.

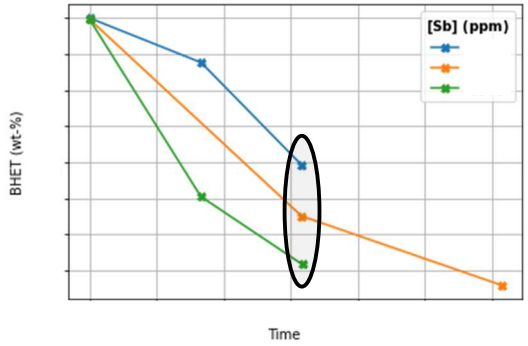

Figure 3-1: BHET VS time and varying [Sb].

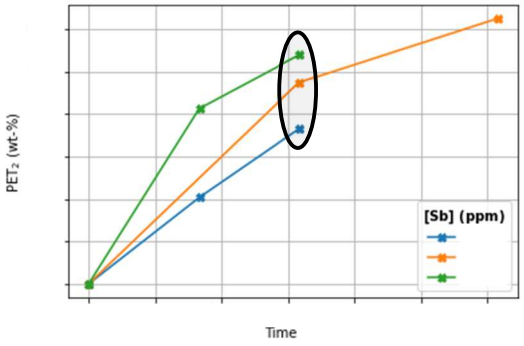

Figure 3-2: PET_2 VS time and varying [Sb].

Figure 3-3 and Figure 3-4 also show three different tests performed at T = 180°C and Sb from MS1%, but at varying [Sb]. Again, it is possible to see a higher rate of conversion of BHET and a higher rate of formation of PET_2 as [Sb] increases. Furthermore, it is also possible to see a clear difference between the results when [Sb] = 0 ppm, *i.e.*, the reaction is uncatalysed, and the results when [Sb] > 0. The uncatalysed reaction proceeds much more slowly than the catalysed reaction, even at small [Sb], which highlights the importance of the use of catalyst in the industrial polymerisation of PET, in order to have a faster and more energy-efficient process.

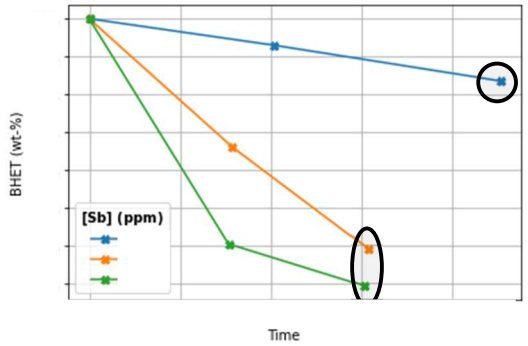

Figure 3-3: BHET VS time and varying [Sb].

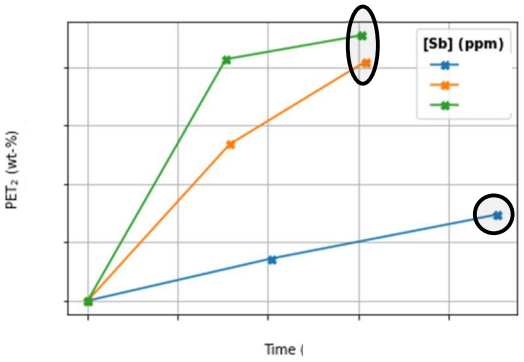

Figure 3-4: PET_2 VS time and varying [Sb].

Finally, Figure 3-5 and Figure 3-6 show three different tests performed at T = 180°C and Sb from MS1%, but at varying [Sb]. The same observations and conclusions can be drawn.

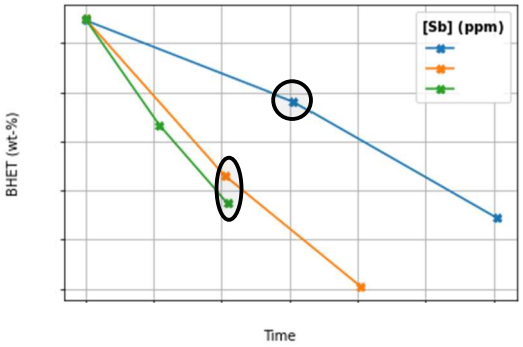

Figure 3-5: BHET VS time and varying [Sb].

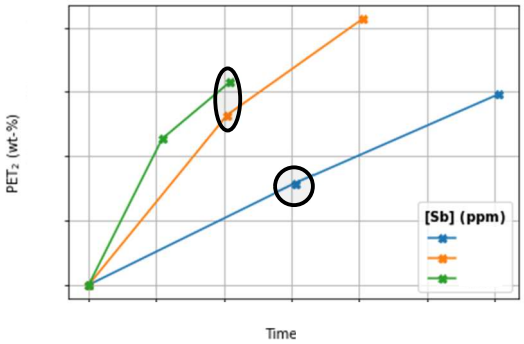

Figure 3-6: PET_2 VS time and varying [Sb].

The figures shown previously do not contain error bars. This was done in order to make their visualisation easier, as the presence of both the error bars and the circles would make the graphs hard to analyse.

3.2 Effect of $BHET_0$:EG_0

The rate of an equilibrium reaction is affected by two factors: the initial concentration of reactants and the driving force for the reaction. In the case of the studied system, the only reactant was BHET, and it was expected that a greater initial concentration of BHET, given by a higher $BHET_0$:EG_0, would mean that there would be initially a higher number of molecules available to react with one another, thus giving a higher initial rate of reaction.

At the same time, the driving force for the reaction is given by the magnitude of Δ_rG, which is translated by a bigger difference between K and K_{eq}, *i.e.*, when $BHET_0$:EG_0 is further away from the equilibrium composition, $BHET_{eq}$:EG_{eq}. The value of K_{eq} is only affected by a change in temperature, so $BHET_{eq}$:EG_{eq} will be the same no matter what $BHET_0$:EG_0 is used, given that the reactions were carried out at the same temperature. Furthermore, polymerisation reactions are approximately athermal, so K_{eq} will not be affected by temperature either.

It was observed that $BHET_{eq}$:EG_{eq} was inferior to all of the $BHET_0$:EG_0 attempted, which means that, as $BHET_0$ increases, both the probability of successful collisions between reactant molecules and the magnitude of Δ_rG increase, so that the rate of reaction is also expected to increase. For the system studied, there is also another factor which is affected by $BHET_0$:EG_0, and that is the inhibition of the catalytic activity of Sb by EG. The greater EG_0, translated by a smaller $BHET_0$:EG_0, the greater the inhibition effect is expected to be, which also means a smaller rate of reaction.

All of these factors lead to the expectation that, as $BHET_0$ increases, *i.e.*, $BHET_0$:EG_0 increases, the rate of reaction will also increase. However, the effect of $BHET_0$:EG_0 on the rate of reaction is not as clear from the experimental results as that of [Sb] and T. Figure 3-7 and Figure 3-8 show three different tests performed at constant [Sb], with Sb from MS1%, and at T=180°C, but at varying $BHET_0$:EG_0. It is possible to observe that both $Conv_{BHET}$ and v_{PET_2} increase when EG_0 is increased.

This result is contrary to expectation, because a smaller $BHET_0$ would mean less reactant molecules at the beginning of the reaction, thus decreasing both the probability of successful collisions between

reactant molecules and also the magnitude of $\Delta_r G$, due to the initial value of K being closer to K_{eq}. This deviation between the experimental result and what was expected initially may be due to uncertainty in analysis and experimental error.

However, it is possible to see that both $Conv_{BHET}$ and v_{PET_2} are significantly smaller for high EG_0 content. This result is expected, given the low value of $BHET_0$ (lower probability of collision between reactant molecules and smaller driving force), and also given the high EG_0, which is expected to greatly inhibit the catalytic activity of Sb.

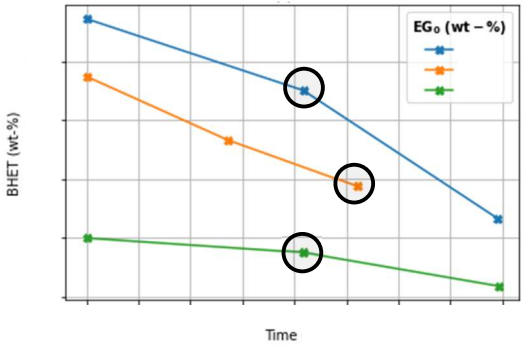

Figure 3-7: BHET VS time and varying EG_0.

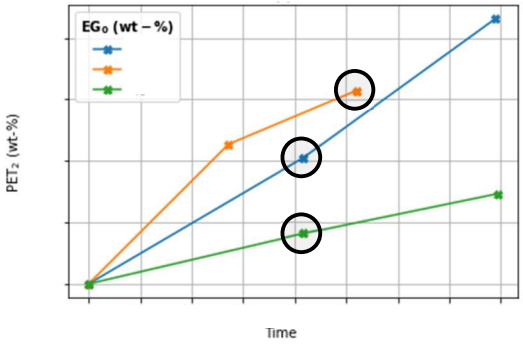

Figure 3-8: PET_2 VS time and varying EG_0.

Figure 3-9 and Figure 3-10 show two different tests performed at constant [Sb], with Sb from MS1%, and at T=180°C, but at varying $BHET_0$:EG_0. It is possible to observe that both $Conv_{BHET}$ and v_{PET_2} decrease when EG_0 is increased, which is expected, given that a higher EG_0 means a smaller probability of successful collisions between reactant BHET molecules, and also a smaller $\Delta_r G$. A higher EG_0 would increase the inhibition on the catalytic activity of Sb. These factors would cause the rate of reaction to decrease. These were the only two tests performed with this high amount of [Sb], and it would be interesting to have another test performed at the same [Sb], but with a different $BHET_0$:EG_0 to see if these results are consistent.

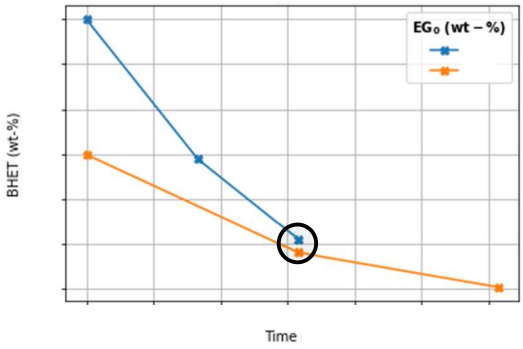

Figure 3-9: BHET VS time varying EG_0.

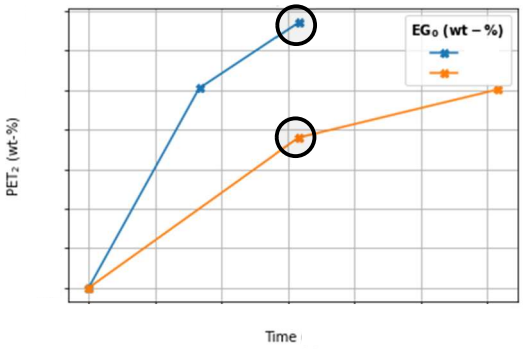

Figure 3-10: PET_2 VS time and varying EG_0.

Figure 3-11 and Figure 3-12 show other three tests performed at constant [Sb], with Sb from MS1%, and at T=180°C, but at varying $BHET_0$:EG_0. This set of results is even more confusing, due to the fact that the values of $BHET_0$:EG_0 for all three sets of experiments are very close, and [Sb] is also relatively small.

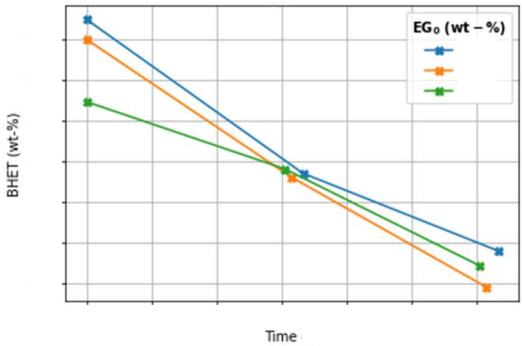

Figure 3-11: BHET VS time and varying EG_0.

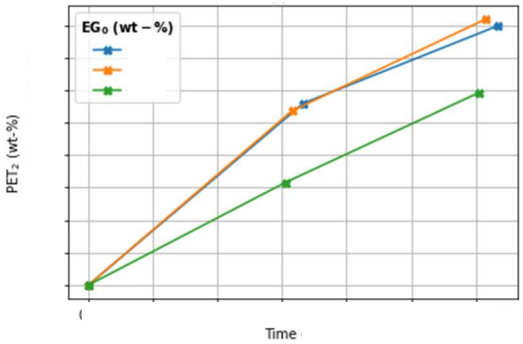

Figure 3-12: PET_2 VS time and varying EG_0.

From these results, it is only possible to conclude that it is difficult to compare sets of experiments whose initial concentrations are different.

3.3 Effect of temperature

As for [Sb], it is easy to observe the effect of temperature on the rate of reaction, because by keeping $BHET_0$:EG_0 constant, the driving force for the reaction remains constant. Figure 3-13 and Figure 3-14 show the change in the amounts of BHET and PET_2 for three different tests performed at constant $BHET_0$:EG_0, constant [Sb] and MS1% as the source of catalyst, but with varying the temperature.

It is clearly visible that an increase in temperature also leads to an increase in the rate of reaction, as both $Conv_{BHET}$ and v_{PET_2} increase with an increase in temperature. A higher temperature means that a higher number of molecules will have enough energy to give successful collisions, which lead to a reaction, which translates in a greater rate of reaction.

However, there is a slight disagreement between the graph showing the evolution of the mass fraction of BHET with time and that showing the evolution of the mass fraction of PET_2. In the former, the test performed at 180°C shows a closer behaviour to that performed at 170°C, while in the latter, the test performed at 180°C shows a closer behaviour to that performed at 190°C.

This result may be due to uncertainties in analysis. It could also be due to constant oscillations in temperature of the dry bath around the set-point values (170°C, 180°C and 190°C), given that the temperature correction performed did not include a correction due to these oscillations. Another possible explanation is the non-homogeneity of the temperature on the different positions of the dry bath heater. As there were only two thermocouples available for the temperature measurements, it was not possible to know the exact temperature inside each individual glass reactor. It was possible that the temperature in some positions of the dry bath heater deviated from the set-point temperatures of the dry-bath heater by significant amounts, which could cause the reaction inside those specific reactors to proceed at different rates than that expected at the set-point temperature.

Both explanations are unlikely because, had them been the case, the effect on $Conv_{BHET}$ and v_{PET_2} would be the same, meaning that they would both increase or decrease due to this temperature oscillation. This was not what was observed, which leads to the conclusion that this result was probably due to uncertainties in analysis.

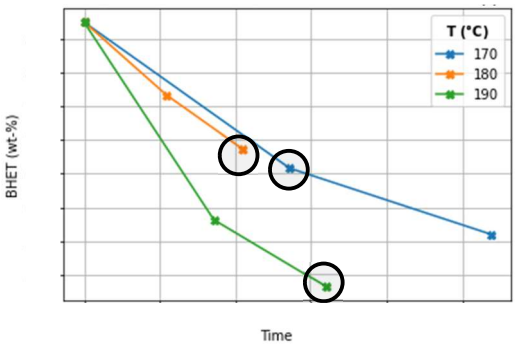

Figure 3-13: BHET VS time and varying temperature.

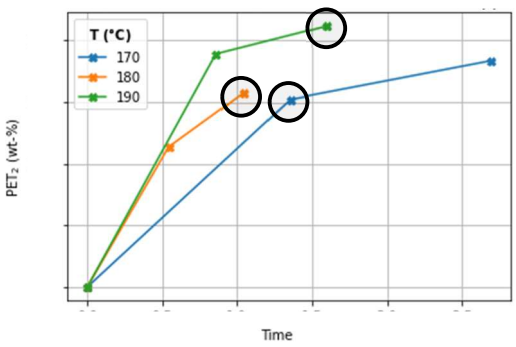

Figure 3-14: PET_2 VS time and varying temperature.

3.4 Repeatability

As mentioned in Section 2.3.5.3, the relative uncertainty in the analysis is ±10%. However, human error in the preparation of the reactors and in carrying out the reactions at constant temperatures, as mentioned in Sections 3.3, could have also affected the experimental results and their reproducibility. For this reason, it was important to repeat some experiments in order to verify the role that these human errors play, if the repeated experiments fall withing each other's range of analytical uncertainty, and if the experiments are reproducible.

Two sets of reactions were repeated in order to confirm the results obtained. The first set of experiments which was chosen to be repeated was one with low EG_0 content and low [Sb] content. When first performed and the results from analysis were received, it was observed that the reaction seemed to reach equilibrium too quickly, *i.e.*, the concentrations of the different species inside the reactor stabilised in a short time. For this reason, this experiment was repeated, using the same reaction conditions and stopping the reaction at the same times.

The comparison between the evolution of the reaction between the first and second run is shown in Figure 3-15. Indeed, it is possible to see that, in the second run, the reaction did not stabilise over the three hours during which it took place, like what happened in the first run. As visible from the error bars, however, the quantifications at 1.5 h fell inside each other's uncertainty intervals, so analytical uncertainty could have played a key role in the observed uncertainty. The values at 3 h, however, do not. As mentioned previously, this set of reactions was chosen to be repeated due to its strange behaviour when first carried out, which might mean that its first run presented anomalous results, which should not be taken into consideration. In order to verify this, it was important to verify the second run of the other set of reactions.

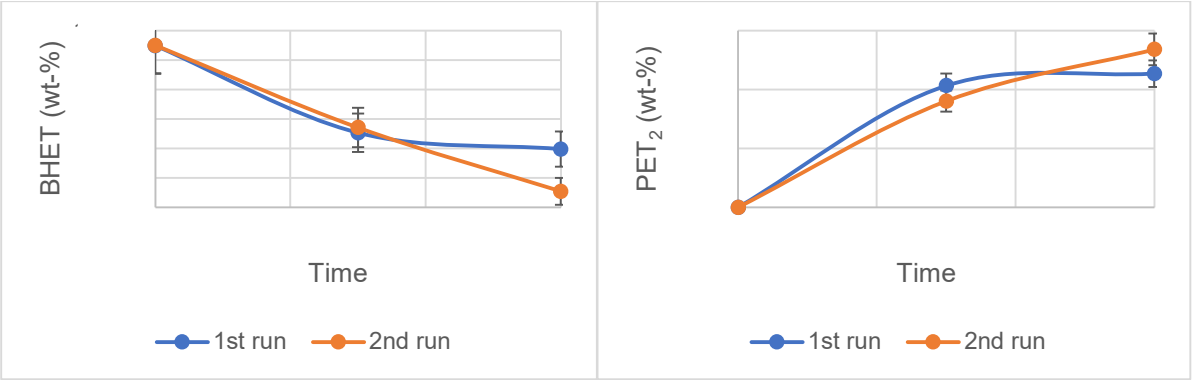

Figure 3-15: Comparison of results obtained in both runs of the experiment with low EG_0 and [Sb] contents.

The other set of experiments which was repeated was one with medium EG_0 and [Sb] contents. This set of experiments had both the highest [Sb] and the highest EG_0, and presented the highest rate of reaction of all experiments carried out on that run. As will be described in Section 3, [Sb] and EG_0 are expected to have opposite effects on the rate of reaction, so the experiment was repeated in order to see if the results obtained were reproducible. In the second run, the reaction was carried out over a longer period of time than in the first run (4,5 h as opposed to 3 h), and the results are shown in Figure 3-16. It is possible to see that they fall within each other's experimental uncertainties and show a more similar trend than those in Figure 3-15, suggesting that the first run of the set of reactions shown in Figure 3-15 was indeed an anomaly, and that it should ne be taken into account for the modelling part, which will be described in Section 4.

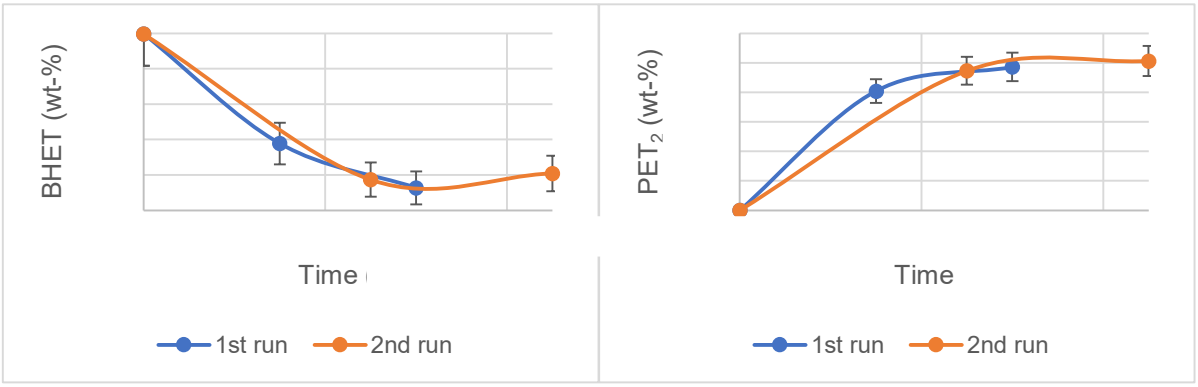

Figure 3-16: Comparison of results obtained in both runs of the experiment with medium EG_0 and [Sb]contents.

4 Modelling

4.1 Model construction hypotheses

Due to the small volume of the reactor and the high agitation, it was assumed that it followed, in the present work, the behaviour of a perfectly batch stirred tank reactor (BSTR). The mass balance for each species, *i*, is given by Equation XIII, where *j* represents each reaction where *i* is present (both the forward, $j \rightarrow$, and the backward, $\leftarrow j$, reaction), r_j is the rate of reaction *j*, $\nu_{i,j}$ is the stoichiometric coefficient of species *i* in reaction *j* and V_R is the volume of the system.

$$\forall_i : \frac{1}{V_R} \times \frac{dn_i}{dt} = \sum_j \nu_{i,j} \times r_j \qquad \text{XIII}$$

The reactions take place in liquid phase, so a constant volume can be assumed. The general form of the mass balance for a constant volume BSTR is given by Equation XIV, in terms of concentration.

$$\forall_i : \frac{d[i]}{dt} = \sum_j \nu_{i,j} \times r_j \qquad \text{XIV}$$

By considering the rate equations presented in Section 1.7, the mass balances for each of the species present in the system of the current work are given in Table 4-1.

Table 4-1: Mass balances for all species considered in the model.

$\frac{d[EG]}{dt} = r_1 + r_2 + r_3 + r_4$	$\frac{d[BHET]}{dt} = -2 \times r_1 - r_2 - r_3$	$\frac{d[PET_2]}{dt} = r_1 - r_2 - 2 \times r_4$
$\frac{d[PET_3]}{dt} = r_2 - r_3$	$\frac{d[PET_4]}{dt} = r_3 + r_4$	

4.2 Equilibrium constant, K_{eq}

As the reaction proceeds, $[Q_q]$ and $[P_p]$ also change and approach their equilibrium values, $[Q_q]_{eq}$ and $[P_p]_{eq}$. For this reason, the value of K will also change and approach its equilibrium value, K_{eq}, also known as the equilibrium constant, whose formula is given by Equation VI. For this reason, in order to calculate K_{eq} from experimental results, it is necessary to carry out reactions until equilibrium, *i.e.*, the state in which $[Q_q]$ and $[P_p]$ have no net change over time

In the present work, however, the reactions were stopped while the system was still in the kinetic regime, *i.e.*, $[Q_q]$ and $[P_p]$ were still varying with time and, for this reason, the values of K_{eq} could not be estimated from these experimental results. For this reason, it was necessary to rely on experimental data obtained in previous work at IFPEN, which involved similar systems and in which the reactions were carried out until equilibrium.

Several repolymerisation tests had been carried out previously at IFPEN under similar reaction conditions using a type of batch reactor. These reactors allow for the employment of higher temperatures

and pressures than the glass reactors used in the current work. Furthermore, these reactions were carried out for longer periods of time (between 6 to 24 hours) and, by plotting the results obtained in those polymerisation tests, it was possible to observe that many of the reactions reached equilibrium at the end of their respective reaction times.

For this reason, it was possible to calculate the values of K_{eq} for each of the reactions shown in the figures above by using the concentrations at the end of the reaction times. The tests carried out ,which were selected in order to calculate the values of K_{eq}, are shown in Table 4-2, along with the temperature at which the reactions were carried out, the duration of time and $BHET_0$:EG_0. Some of these reactions initially had some short-chain oligomers of PET in addition to BHET and EG.

Table 4-2: Temperature, reaction time and $BHET_0$:EG_0 of each selected test performed.

Test #	1	2	3
T (°C)	205	205	205
Time (h)	24	6	6
$BHET_0$:EG_0			

Since it can be considered that polymerisation reactions are approximately athermal and thus that their K_{eq} does not vary with temperature, the values of K_{eq} calculated from the reactions carried out in the batch reactor were not modified. These values of K_{eq} obtained for each of the tests considered in Table 4-2 are shown in Table 4-3.

Table 4-3: Values of K_{eq} for each of the four equilibrium reactions considered, for each of the selected tests.

Test #	1	2	3
K_{eq_1}			
K_{eq_2}			
K_{eq_3}			
K_{eq_4}			

Due to difficulties in solubility of PET_3 and PET_4 in THF at room temperature, the values of K_{eq} for the reactions involving those species, i.e., K_{eq_3} and K_{eq_4}, were considered as equal to 1, which corresponds to an average of the literature values and is coherent with the stability of organic functions during transesterification (esters of glycol into similar esters of glycol). For K_{eq_1} and K_{eq_2}, an average of the IFPEN experimental values highlighted in green and yellow, respectively, was calculated. By using this approach, the values of K_{eq_1} and K_{eq_2} calculated were 0.9 and 1.6, respectively.

Table 4-4: Final values of K_{eq} for each of the four equations considered.

K_{eq_1}	K_{eq_2}	K_{eq_3}	K_{eq_4}

4.3 Inhibition formalism

The reaction rate constant of a catalysed reaction, k, can be split into a noncatalytic (thermal) term, k^{th}, and a catalytic term, $k^{cat'}$. Both terms are dependent on the temperature of the system, but $k^{cat'}$ may also be dependent on several other factors, such as [Sb], [EG] and other parameters (α_1, α_2, …), depending on how it is defined. Furthermore, given that the reactions taking place in the current system are

reversible reactions, the reaction rate constants considered were the ones relative to the forward reactions, $k_{j\rightarrow}$, as shown in Equation XV.

$$k_{j\rightarrow}(T) = k_{j\rightarrow}^{th}(T) + k_{j\rightarrow}^{cat'}\left(T, [Sb], [EG], \alpha_{1_j}, \alpha_{2_j}, \dots\right) \quad \text{XV}$$

By defining a formalism for the catalytic activity of Sb, $\mathcal{FM}$, which may take into account both its catalytic activity and the inhibition effects on it, it is possible to decorrelate the $k^{cat'}$ term into a part which is only dependent on the temperature, k^{cat}, and a part which is dependent on other parameters, $\mathcal{FM}$, as is shown in Equation XVI.

$$k_{j\rightarrow}(T) = k_{j\rightarrow}^{th}(T) + k_{j\rightarrow}^{cat}(T) \times \mathcal{FM}\left([Sb], [EG], \alpha_{1_j}, \alpha_{2_j}, \dots\right) \quad \text{XVI}$$

Fitting one different $k_{j\rightarrow}$ for each reaction *j*, all with their individual $k_{j\rightarrow}^{th}$, $k_{j\rightarrow}^{cat}$ and other parameters, would require an extremely sensitive database, which would come from experiments carried in a carefully controlled environment, and whose results were analysed with extremely sensitive analytical techniques, capable of identifying every species present. Attempting to fit all these individual parameters for each reaction would cause great correlation and interdependency between these parameters, which would render their estimation difficult. For this reason, only one rate constant for the forward reaction for all four reactions was considered, with only one set of parameters to fit. Rewriting Equation XVI gives Equation XVII.

$$k(T) = k^{th}(T) + k^{cat}(T) \times \mathcal{FM}([Sb], [EG], \alpha_1, \alpha_2, \dots) \quad \text{XVII}$$

By considering a reference temperature, T_{ref}, it is possible to remove the temperature dependency from k^{th} and k^{cat}, by introducing the Arrhenius equation, thus obtaining k^{th} and k^{cat} at T_{ref}, *i.e.*, k_{ref}^{th} and k_{ref}^{cat}. This would also allow for an estimation of E_a. The resulting expression is shown in Equation XVIII. The terms shown in bold are the terms which could be estimated from the experimental results. It should be noted that Equation XVIII considers E_a as the same for both k^{th} and k^{cat}. *i.e.*, equal for the uncatalysed and for the catalysed reactions. This was a simplification made, again, due to the nature of the database and to prevent a strong correlation between the tuned parameters.

$$k(T) = \left\{\mathbf{k_{ref}^{th}} + \mathbf{k_{ref}^{cat}} \times \mathcal{FM}([Sb], [EG], \boldsymbol{\alpha_1}, \boldsymbol{\alpha_2}, \dots)\right\} \times \exp\left(-\frac{\mathbf{E_a}}{R}\left[\frac{1}{T} - \frac{1}{T_{ref}}\right]\right) \quad \text{XVIII}$$

Not all sets of experimental results shown in were used in order to fit the parameters of the model, because some of the results were not available soon, and it was necessary to begin the modelling work before their availability. For this reason, some experimental results were used as a fitting database, which was used to tune the parameters, and others as a validation database, which were obtained after the parameters were tuned in order to validate the formalism.

4.4 Formalisms from literature

As mentioned in Section 1.6, Yamada and Duh *et al.* proposed that k is directly proportional to [Sb], while Hovenkamp proposed that k is directly proportional to [Sb], but inversely proportional to 1+φ[EG],

where φ is a constant. These are two different correlations that attempt to explain how different factors influence the rate of reaction. These correlations can be adapted and substituted in Equation XVIII, as the $\mathcal{FM}$ part.

Despite having carried out the experimental work at different temperatures and pressures, in different types of reactors, using different volumes, and using different concentrations of reactant and catalyst, it is expected that the correlations proposed by these authors still be applicable to the system studied in the current thesis, as both involve the polymerisation of PET and use the same reactants. However, some deviation is still expected.

4.4.1 Yamada formalism

By considering the correlation proposed by Yamada and Duh *et al.*, $\mathcal{FM}$ was considered as equal to [Sb]. The resulting expression for k is shown in Equation XIX, where the parameters to be fitted are highlighted in bold.

$$k(T) = \left\{\mathbf{k_{ref}^{th}} + \mathbf{k_{ref}^{cat}} \times [Sb]\right\} \times \exp\left(-\frac{\mathbf{E_a}}{R}\left[\frac{1}{T} - \frac{1}{T_{ref}}\right]\right) \quad \text{XIX}$$

4.4.2 Hovenkamp formalism

By considering the correlation derived from Hovenkamp, the resulting expression for k is given by Equation XX. The additional parameter k_{inh} is equivalent to the term φ shown previously and it accounts for the inhibition effect of EG on the catalytic activity of Sb.

$$k(T) = \left\{\mathbf{k_{ref}^{th}} + \mathbf{k_{ref}^{cat}} \times \frac{[Sb]}{1 + \mathbf{k_{inh}} \times [EG]}\right\} \times \exp\left(-\frac{\mathbf{E_a}}{R}\left[\frac{1}{T} - \frac{1}{T_{ref}}\right]\right) \quad \text{XX}$$

4.4.3 Estimation of parameters

4.4.3.1 Methodology

The softwares used in the current work are Python 3 (in Jupyter interface) and AthenaVisual Studio (AVS), which uses Fortran language.

Firstly, the experimental data was fed to both Python and AVS and the reactor models, with all the chemical species and mass balances, with each formalism, were defined on both of them.

Secondly, the behaviour of the model and the effects of the different parameters to be fitted from each formalism were studied on Python, in order to carry out sensibility analyses and choose first guesses of the values of each parameter.

Thirdly, these first guesses of the parameters were added to the model on AVS, where they were tuned to fit the experimental results as best as possible. Apart from the optimised parameters, AVS also returned t he t-value, standard deviation and 95% confidence interval for each of the optimised parameters.

Lastly, the parameters optimised on AVS were added back to the model on Python, and the final graphs were plotted, in order to see how the model with the optimised parameters would fit to the experimental results, by obtaining the t-value, standard deviation (SD) and confidence interval (CI). Parity plots and residual graphs were also plotted to observe the tendencies of the model.

4.4.3.2 Results

4.4.3.2.1 Yamada formalism

The parameters fitted are shown in Table 4-5. The performance of experiments without the presence of catalyst allowed for the tunning of k_{ref}^{th}. Two experiments were performed without adding catalyst, and these were the ones used for the tuning of k_{ref}^{th}. The performance of experiments at varying catalyst concentrations allowed for the tunning of k_{ref}^{cat}. Only the experiments in which MS1% was used as the precursor of catalyst and those on which EG_0 was low were used for the tunning of k_{ref}^{cat}, as will be explained forward. Finally, the performance of experiments at different temperatures allowed for the tuning of E_a.

The tuned values of each of these parameters, with the respective t-value, standard deviation (SD) and confidence interval (CI) are shown in Table 4-5.

Table 4-5: Tuned parameters in the Yamada formalism.

Paramater	Value	t-value	SD	95% CI	Final values
$\mathbf{k_{ref}^{th}}$		16.3			
$\mathbf{k_{ref}^{cat}}$		47.9			
$\mathbf{E_a}$	96.2	8.17	2.93	6.14	96±6 kJ/mol

Figure 4-1, Figure 4-2, Figure 4-3 and Figure 4-4 show different graphs depicting how well the reactor model with the Yamada formalism fit a few different sets of experimental results. Given that this formalism does not consider that EG inhibits the catalytic effect of Sb, it is interesting to look how well it fit the experimental results over the entire range, to see for which ranges of EG_0 and [Sb] it is most applicable.

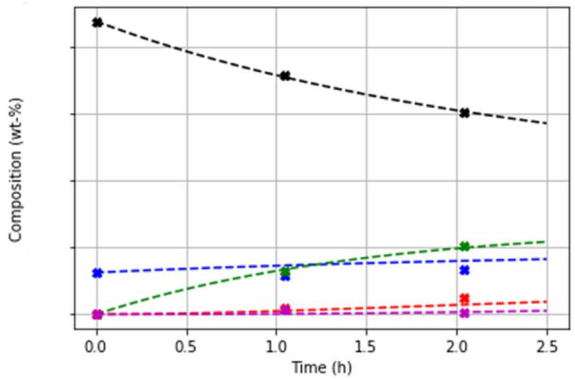

Figure 4-1: condition 1;R^2=0.99.

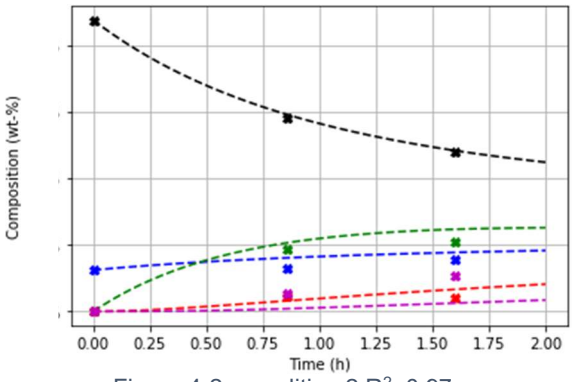

Figure 4-2: condition 2;R^2=0.97.

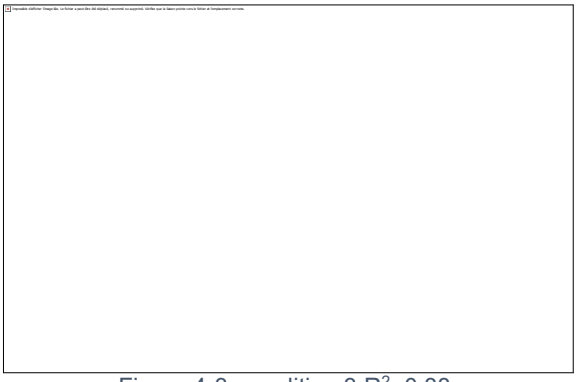

Figure 4-3: condition 3;R^2=0.88.

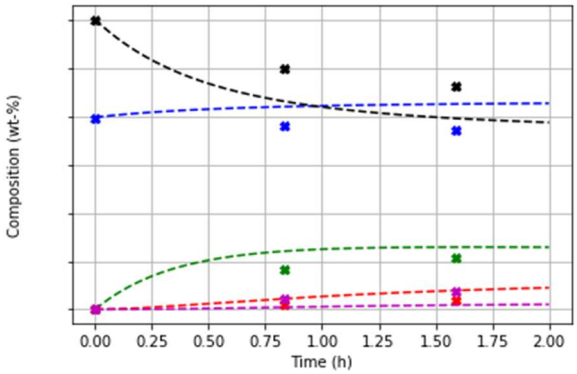

Figure 4-4: condition 4;R^2=0.45.

4.4.3.2.2 Hovenkamp formalism

The parameters fitted are shown in Table 4-6. It should be noted that only the value of k_{inh} was fitted for the Hovenkamp formalism, while the values of k_{ref}^{th}, k_{ref}^{cat} and E_a shown in Table 4-6 were the same as the ones which were fitted with the Yamada formalism, shown in Table 4-5. The new parameter was tuned with the experiments in which EG_0 was higher, which will be explained later.

Table 4-6: Tuned parameters in the Hovenkamp formalism.

Paramater	Value	t-value	SD	95% CI	Final values
$\mathbf{k_{ref}^{th}}$		16.3			
$\mathbf{k_{ref}^{cat}}$		47.9			
$\mathbf{E_a}$	96.2	8.17	2.93	6.14	96±6 kJ/mol
$\mathbf{k_{inh}}$		29.7			

Figure 4-5, Figure 4-6, Figure 4-7 and Figure 4-8 show different graphs which show how well the reactor model with the Hovenkamp formalism fit a few different sets of experimental results. Given that this model does consider that EG inhibits the catalytic activity of Sb, it is most interesting to see how well it fits to the experiments performed at higher EG_0, which is the range of values at which inhibition is likely to be present. However, it is also necessary to see if the addition of the parameter k_{inh} into the model makes it less applicable to the experiments with lower EG_0.

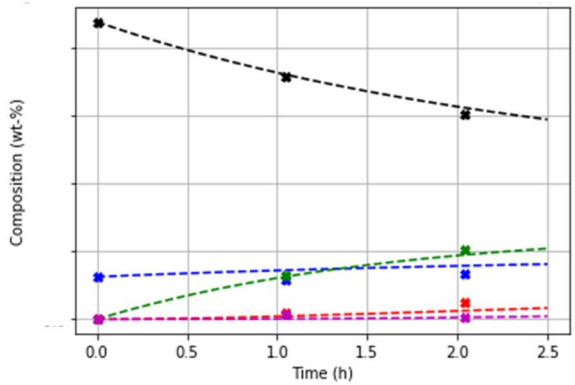

Figure 4-5: condition 1;R^2=0.97.

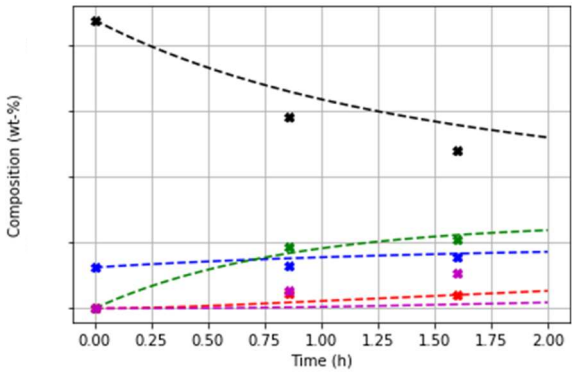

Figure 4-6: condition 2;R^2=0.92.

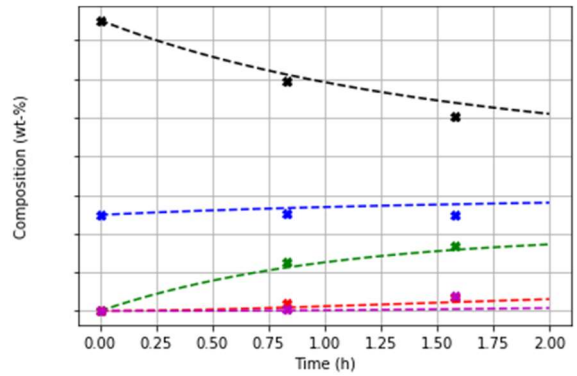

Figure 4-7: condition 3;R^2=0.95.

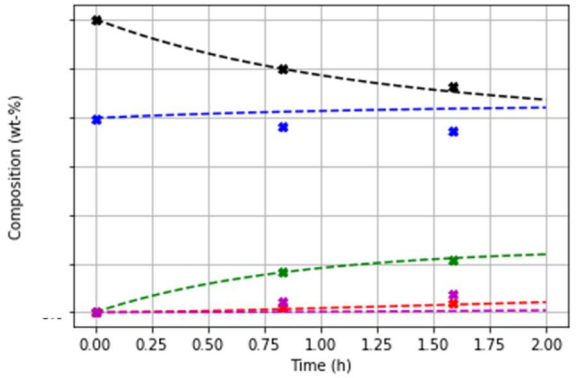

Figure 4-8: condition 4;R^2=0.99.

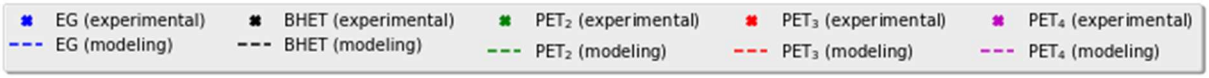

4.4.3.2.3 Remarks

By looking at the values of R^2 from the graphs, it is possible to see that the Yamada formalism showed a good fitting to the experimental results (R^2 above 0.95) when EG_0 was low *ca.*, but a much inferior response when EG_0 was equal or above that value. This is due to the fact that this formalism does not consider that EG inhibits the catalytic activity of Sb, hence, considering that this inhibition takes place in the real system, it is possible to infer that this formalism is only applicable when this effect is negligible, *i.e.*, when the amount of EG present is low.

The Hovenkamp formalism, on the other hand, does consider the inhibitory effect of EG and, for this reason, presents a much superior behaviour to the Yamada formalism when EG_0 is above and equal to *ca.* 25 wt-%, *i.e.*, when the inhibitory effect is not negligible due to the high amount of EG present in the system. This superior behaviour is reflected in the higher values of R^2 for experiments in that range. However, this formalism presents, on average, an inferior fitting to the experimental results for the sets of experiments in which EG_0 is below *ca.* 25 wt-%.

The 25 wt-% value was considered because, as mentioned previously, sensitivity analyses were performed on Python before tunning the parameters. One of these sensitivity analysis involved tuning by hand an optimal value of k^{cat} for each individual set of experiments. Figure 4-9 shows each of those tuned values of k^{cat} , for the experiments in the fitting database, as a function of EG_0 of the respective set. However, it clear that k^{cat} shows a negative trend with increasing EG_0 for all ranges of EG_0 shown.

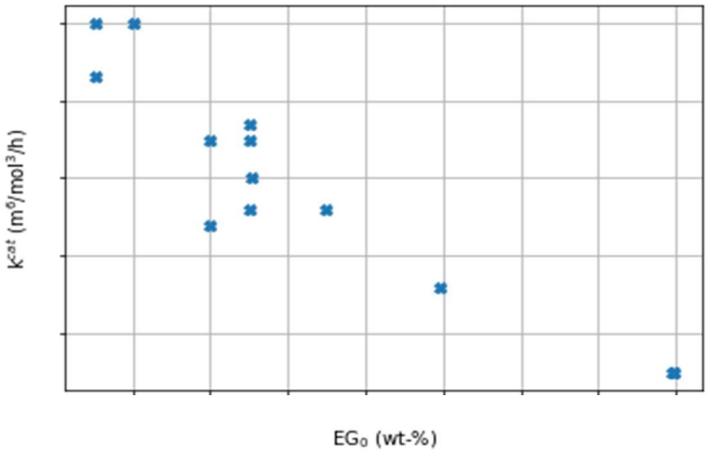

Figure 4-9: Tuned values of k^{cat} as a function of EG_0 of the respective set.

In order to further compare the two formalisms from literature, it was interesting to first look at the parity plots for BHET and PET_2 for all three formalisms. In Figure 4-10 and Figure 4-11which show the parity ploits for the Yamada formalism, it is possible to see a weaker correlation when the amount of BHET in solution was low (which automatically means that the amount of EG was high), and this further emphasises the limitation of the Yamada formalism for high EG_0. For lower values of EG_0, however, this formalism presents a good behaviour, due to the inhibitory effect of EG being negligible.

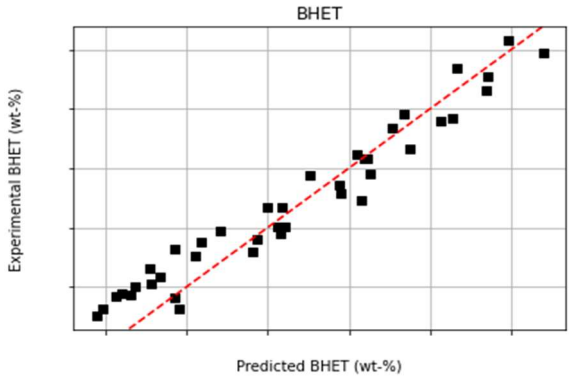

Figure 4-10: Parity plot for BHET in Yamada formalism.

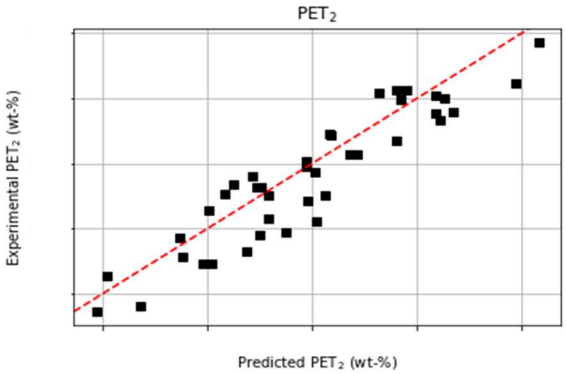

Figure 4-11: Parity plot for PET_2 in Yamada formalism.

In Figure 4-12 and Figure 4-13, which show the parity plots for the Hovenkamp formalism, it is possible to see that, although there is a storng correlation for low values of BHET (and high high values of EG) and PET_2, this correlation is much weaker for intermediary and high values of BHET. This demonstrates that this formalism is much more applicable for higher values of EG_0.

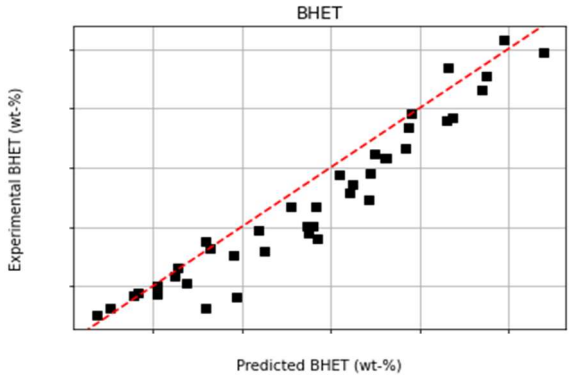

Figure 4-12: Parity plot for BHET in Hovenkamp formalism.

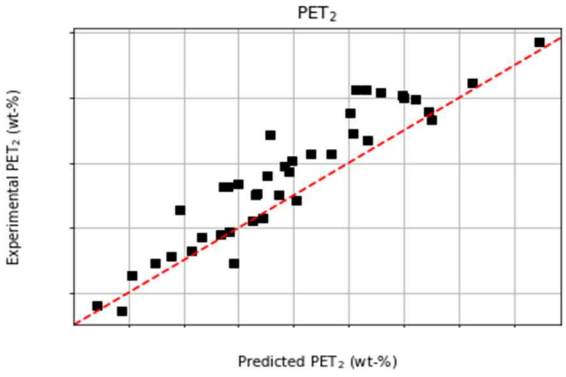

Figure 4-13: Parity plot for PET_2 in Hovenkamp formalism.

Figure 4-14, Figure 4-15, Figure 4-16 and Figure 4-17, which show the BHET and PET_2 residuals for both formalisms as a function of EG_0. In Figure 4-16 and Figure 4-17, it is clear that the residuals are much smaller than in Figure 4-14 and Figure 4-15 for higher values of EG_0, due to taking into account the inhibitory effect of EG, as was shown in the parity plots.

However, the Hovenkamp formalism also shows higher residuals than Yamada for low values of EG_0, which indicates, again, a worse behaviour in that range. This is due to a conflict between the sets of values chosen to fit k_{ref}^{cat} and k_{inh}, respectively. The parameter k_{ref}^{cat} was tuned with sets of experiments carried out at EG_0 below 25 wt-%, while k_{inh} was tuned with sets of experiments carried out at EG_0 above 17.5 wt-%. This difference might explain the worse behaviour of the Hovenkamp formalisms for low values of EG_0, and the inability of both formalisms from literature to accurately predict the behaviour of the system at all ranges studied.

For this reason, a challenge still remained, and that was to propose a formalism which was able to overcome the constraints posed by both formalisms, *i.e.*, a formalism which was applicable over the entire range of EG_0 studied in the current work.

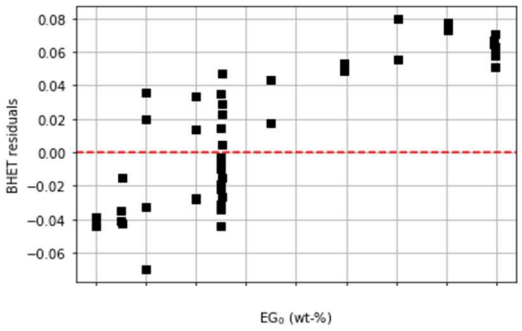

Figure 4-14: BHET residuals VS EG_0 for Yamada formalism.

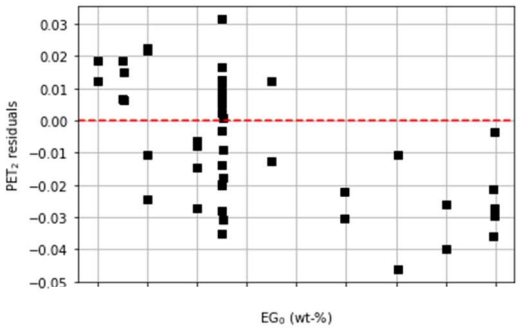

Figure 4-15: PET_2 residuals VS EG_0 for Yamada formalism.

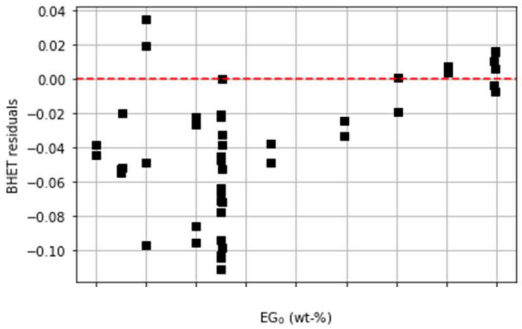

Figure 4-16: BHET residuals VS EG_0 for Hovenkamp formalism.

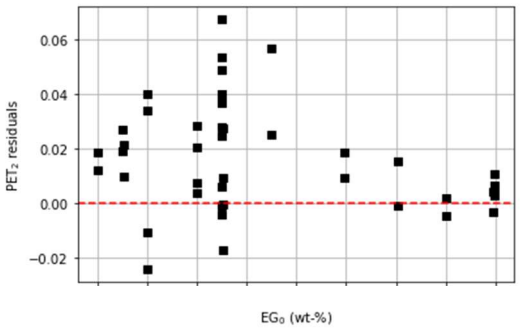

Figure 4-17: PET_2 residuals VS EG_0 for Hovenkamp formalism

4.5 Proposed formalism

4.5.1 Apparent kinetics

In order to propose a new formalism for the catalytic activity of Sb, it was necessary to look at the apparent kinetic rate constant of the reaction, k^{app}, and see how this parameter is affected by [Sb] and [EG] individually. In the method followed previously, k was split into k^{th} and $k^{cat'}$ and, by also taking $\mathcal{FM}$ and the Arrhenius equation into account, the parameters to be fitted were k^{th}_{ref}, k^{cat}_{ref}, E_a and k_{inh} (for the Hovenkamp formalism).

When considering the apparent kinetics of the reaction, only one parameter, k^{app}, was fitted, without splitting it into two parts and taking $\mathcal{FM}$ into account. As in the previous method, only one k^{app} was fitted for all four reversible reactions, *j*, considered. However, since it was desired to observe the effect of [Sb] and [EG] on k^{app}, one k^{app} was fitted individually for each set of experimental results, *z*. By considering that both k^{app} and $k^{cat'}$ are different for each set of experimental results, *z*, while k^{th} is constant, it is possible to rewrite Equation XV in the form shown by Equation XXI.

$$k_z^{app} = k^{th} + k_z^{cat'} \qquad \text{XXI}$$

For this reason, it was possible to write the rate equation for each reaction, *j*, and for each set of experimental results, *z*, as shown in Equation XXII, where *p* and *q* refer to products and reactants, respectively. The value of k_z^{app} can be individually tuned for each set of experimental results, *z*

$$\forall_{z,j}: \quad \mathrm{r}_j = \mathrm{k}_z^{\mathrm{app}} \times \left(\prod\nolimits_{p \in j} [\mathrm{P}_p]^{\nu_p} - \frac{\prod_{q \in j} [\mathrm{Q}_q]^{\nu_q}}{\mathrm{K}_{\mathrm{eq}_j}} \right) \qquad \text{XXII}$$

It is possible to rewrite Equation XXI by putting $k^{cat'}$ in evidence, as shown by Equation XXIII. By this equation, it is possible to obtain a single value of $k^{cat'}$ for each set of experimental results, ***z***, just by knowing k^{app} (tuned individually for each set of experimental results, ***z***) and k^{th} (tuned previously, when obtaining the parameters for the Yamada formalism).

$$\mathrm{k}_z^{\mathrm{cat}\prime} = \mathrm{k}_z^{\mathrm{app}} - \mathrm{k}^{\mathrm{th}} \qquad \text{XXIII}$$

The advantage of using apparent kinetics is that it allows for the calculation of one single value of $k^{cat'}$ for each set of experimental results, ***z***, and without making any assumptions, which was not the case when the formalisms were used. In the Hovenkamp formalism, $k^{cat'}$ was not constant, because it was dependent on [EG], which varied with time for a given set of experimental results, ***z***. In the Yamada formalism, $k^{cat'}$ was not dependent on time, but it was assumed that $k^{cat'}$ was directly proportional to [Sb].

For this reason, using the approach of apparent kinetics would allow for the calculation of a single value of $k^{cat'}$ for each set of experimental results, ***z***, and it would be possible to observe how $k^{cat'}$ is affected by [Sb] and [EG], and then propose a formalism based on these experimental findings. Assuming that $k^{cat'}$ can be decorrelated into two functions, one solely dependent on [Sb], *f*([Sb]), and the other solely dependent on [EG], *g*([EG]), it is possible to obtain Equation XXIV.

$$f([\mathrm{Sb}]) \times g([\mathrm{EG}]) = \mathrm{k}_z^{\mathrm{app}} - \mathrm{k}^{\mathrm{th}} \qquad \text{XXIV}$$

4.5.1.1 *f*([Sb])

The equation *f*([Sb]) can be obtained by considering sets of experimental results where [EG] is kept constant, so that *g*([EG]) is constant, and only [Sb] is allowed to vary. In order to achieve this, both sides of Equation XXIV were divided by *g*([EG]), thus giving Equation XXV.

$$f([\mathrm{Sb}]) = \frac{\mathrm{k}_z^{\mathrm{app}} - \mathrm{k}^{\mathrm{th}}}{g([\mathrm{EG}])} \qquad \text{XXV}$$

By assuming that *g*([EG]) is given by a rational function, as proposed by the Hovenkamp formalism, it is possible to obtain Equation XXVI.

$$f([\mathrm{Sb}]) = \left(\mathrm{k}_z^{\mathrm{app}} - \mathrm{k}^{\mathrm{th}}\right) \times (1 + \mathrm{k}_{\mathrm{inh}} \times [\mathrm{EG}]) \qquad \text{XXVI}$$

Given that k^{th} and k_{inh} are both constants, which were tuned previously, and that [EG] will also be constant, only k^{app} will vary between the different sets of experimental results, ***z***. This means that plotting the expression on the right-hand side of Equation XXVI as a function of the value of [Sb] of the corresponding set of experimental results, ***z***, it would be possible to observe how k^{app} varies with [Sb].

Figure 4-18, Figure 4-19, Figure 4-20 and Figure 4-21 show this relationship for four different values of EG_0. It is possible to observe that a linear function, given by Equation XXVII, is able to predict well the relationship between k^{app} and [Sb].

$$y(x) = m \times x + c \qquad \text{XXVII}$$

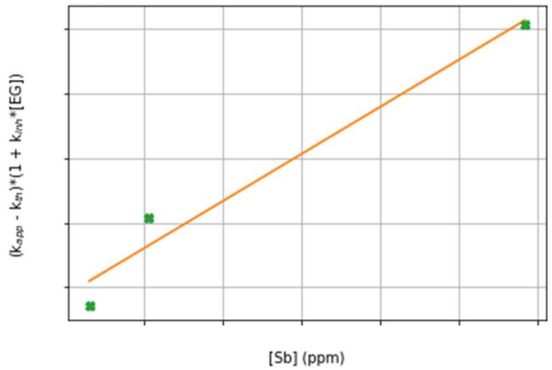

Figure 4-18: condition 1 and R^2=0.97.

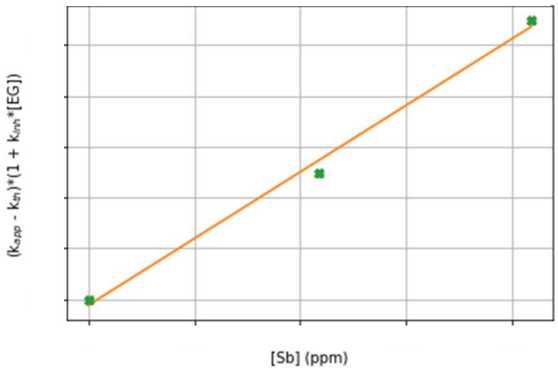

Figure 4-19: condition 2 and R^2=0.99.

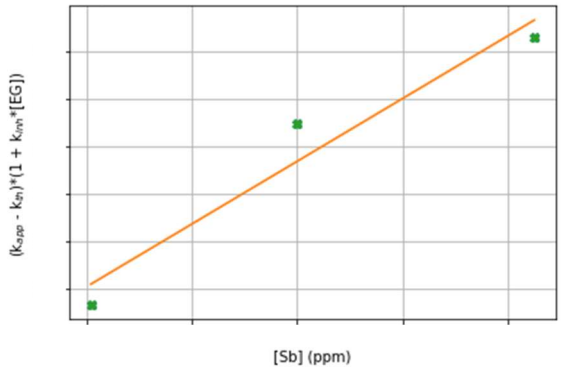

Figure 4-20: condition 3 and R^2=0.94.

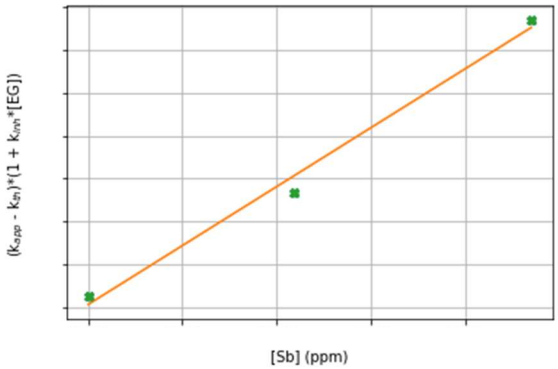

Figure 4-21: condition 4 and R^2=0.99.

This observation suggests that a better formalism would include the term [Sb] inside a first degree polynomial, in the form shown in Equation XXVIII, with nonzero values of α and β, as opposed to α and β equal to 0 and 1, as proposed by both Yamada and Hovenkamp.

$$f([\mathrm{Sb}]) = \alpha + \beta \times [\mathrm{Sb}] \qquad \text{XXVIII}$$

4.5.1.2 *g*([EG])

In the case of *g*([EG]), a very similar approach to *f*([Sb]) was taken, starting by dividing both sides of Equation XXIV by *f*([Sb]), thus giving Equation XXIX.

$$g([\mathrm{EG}]) = \frac{k_z^{app} - k^{th}}{f([\mathrm{Sb}])} \qquad \text{XXIX}$$

By assuming that *f*([Sb]) is simply given by [Sb], as proposed by Yamada and Hovenkamp, it is possible to obtain Equation XXX. It will be shown that a polynomial of degree 1 with nonzero α and β gave a better response. However, these parameters would still need to be fitted, and this fitting would be done afterwards, once seeing how both *f*([Sb]) and *g*([EG]) behaved. For this reason, the approximation *f*([Sb])=[Sb] was done, to see how k^{app} was affected by [EG].

$$g([\mathrm{EG}]) = \frac{k_z^{app} - k^{th}}{[\mathrm{Sb}]} \qquad \text{XXX}$$

Figure 4-22, Figure 4-23 and Figure 4-24 show a plot of the right-hand side of Equation XXX as a function of [EG]. It is possible to see that a rational function, in the form given by Equation XXXI, is able to predict well the relationship between k^{app} and [EG], as proposed by Hovenkamp. Given that less experimental results were available to draw more conclusions, it was considered that *g*([EG]) was as proposed by Hovenkamp, without any additions.

$$y(x) = \frac{1}{c + m \times x} \qquad \text{XXXI}$$

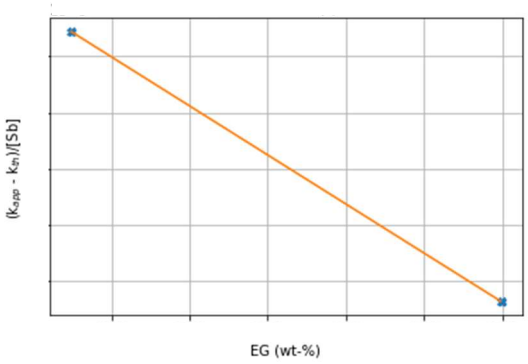

Figure 4-22: condition 1 and R^2=1.00.

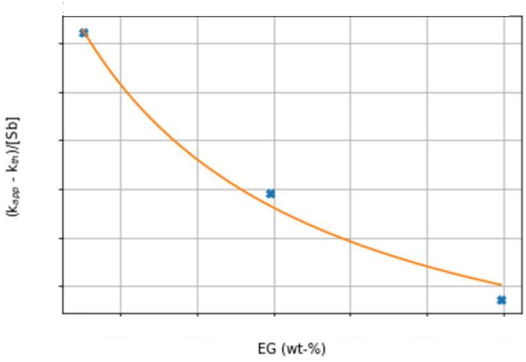

Figure 4-23: condition 2 and R^2=0.99.

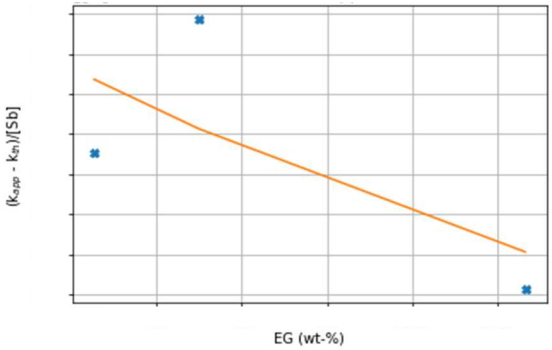

Figure 4-24: condition 3 and R^2=0.48.

4.5.2 Proposed new formalism

Based on the results shown in Section 4.5.1, the final proposed formalism is shown in Equation XXXII, with three extra parameters: α, β and γ.

$$k(T) = \left\{ \mathbf{k_{ref}^{th}} + \mathbf{k_{ref}^{cat}} \times \frac{\boldsymbol{\alpha} + \boldsymbol{\beta} \times [\mathrm{Sb}]}{1 + (\mathbf{k_{inh}} \times [\mathrm{EG}])^{\boldsymbol{\gamma}}} \right\} \times \exp\left(-\frac{\mathbf{E_a}}{R} \left[\frac{1}{T} - \frac{1}{T_{ref}} \right] \right) \qquad \text{XXXII}$$

The parameters α and β were added based on the findings of Section 4.5.1 and the observation of how k^{app} varies with [Sb]. Like for k_{ref}^{cat}, these were tuned using the experimental results for all ranges of EG_0, in attempts to find a model which was able to well predict the behaviour of the model for all experimental conditions. The parameter γ was also added after observing the behaviour of the model with the newly tuned parameters α and β, and then attempting one last modification in order to further improve the

behaviour of the formalism, by using again all sets of experimental results. The tuned parameters are shown in Table 4-7.

Table 4-7: Tuned parameters in the proposed formalism.

Paramater	Value	t-value	SD	95% CI	Final values
k_{ref}^{th}		16.3			
k_{ref}^{cat}		47.9			
E_a	96.2	8.17	2.93	6.14	96±6 kJ/mol
k_{inh}		29.7			
α		-			
β		-			
γ		-			

Figure 4-25, Figure 4-26, Figure 4-27 and Figure 4-28 show different graphs which show how well the reactor model with the proposed formalism fit a few different sets of experimental results. The values of R2 for the two formalisms from literature for the same sets of experiments were also included.

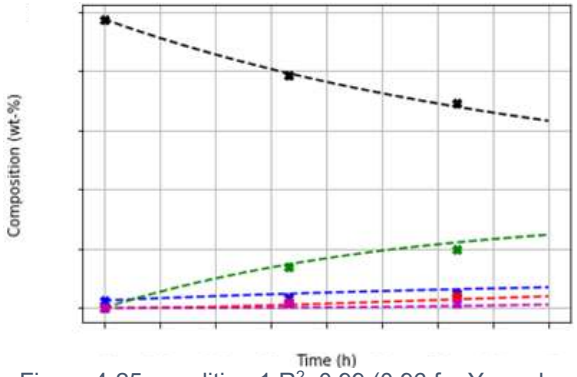

Figure 4-25: condition 1;R^2=0.99 (0.96 for Yamada and 0.92 for Hovenkamp).

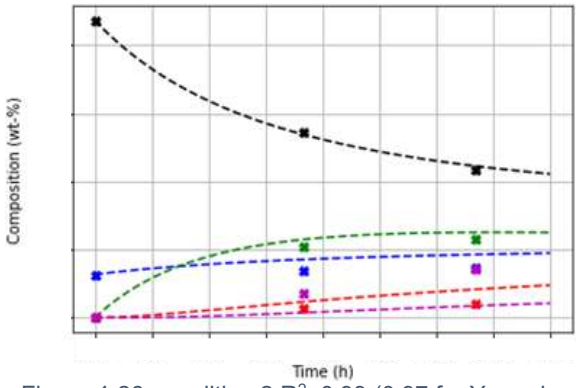

Figure 4-26: condition 2;R^2=0.99 (0.97 for Yamada and 0.98 for Hovenkamp).

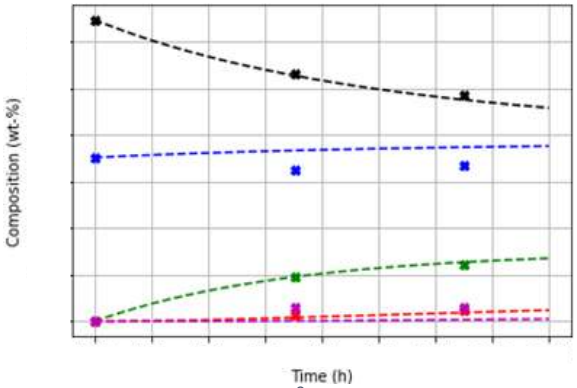

Figure 4-27: condition 3;R^2=1.00 (0.47 for Yamada and 0.70 for Hovenkamp).

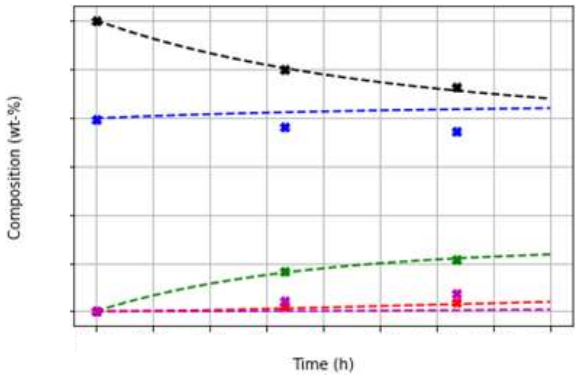

Figure 4-28: condition 4;R^2=0.99 (0.45 for Yamada and 0.99 for Hovenkamp).

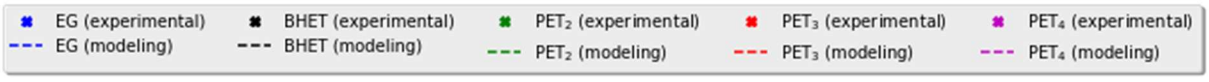

It is possible to see that the values of R^2 for the proposed formalism were above 0.99 and either higher or equal to those of the formalisms from literature. This means that, for nearly all sets of experimental results the proposed formalism, has an equal or better response than those of the formalisms from literature and that the proposed formalism is able to accurately predict the experimental results for all experimental conditions. In order to observe the tendencies of the proposed formalism, the parity plots

and residual graphs for it were also plotted. The parity plots are shown in Figure 4-29 and Figure 4-30, while the residual plots are shown in Figure 4-31 and Figure 4-32.were It is clear that, like the Hovenkamp formalism, the proposed formalism shows a very strong correlation when EG_0 is elevated. However, it is also possible to observe that it shows small residues for lower values of EG_0, as in the case of the Yamada formalism. This allows for the conclusion that the addition of the three extra parameters α, β and γ allowed for a formalism that overcomes the difficulties posed by both formalisms from literature and allowed for a good prediction of the experimental results for all ranges of EG_0 studied in the current work.

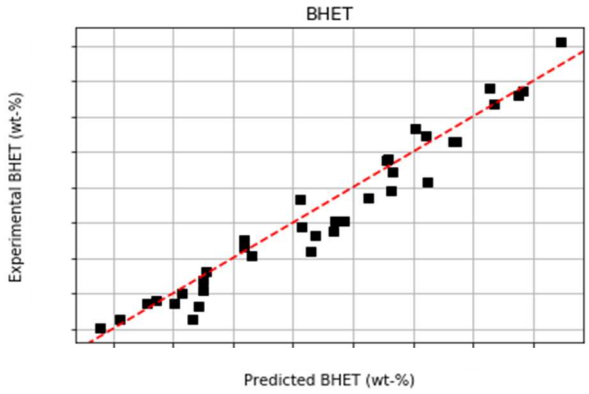

Figure 4-29: Parity plot for BHET in proposed formalism.

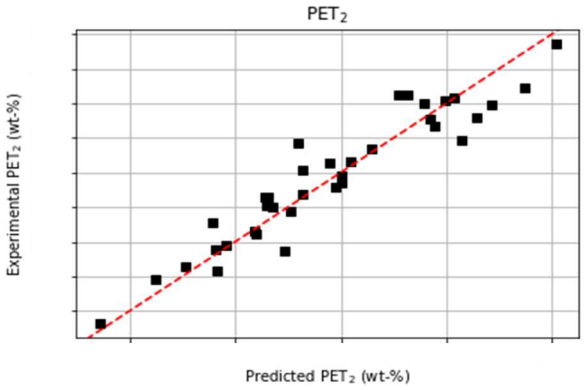

Figure 4-30: Parity plot for PET_2 in proposed formalism.

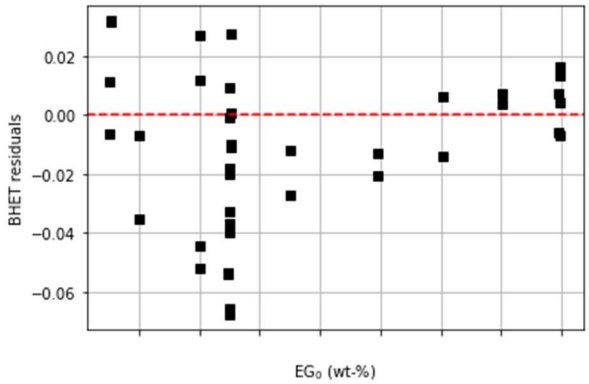

Figure 4-31: BHET residuals VS EG_0 for the proposed formalism.

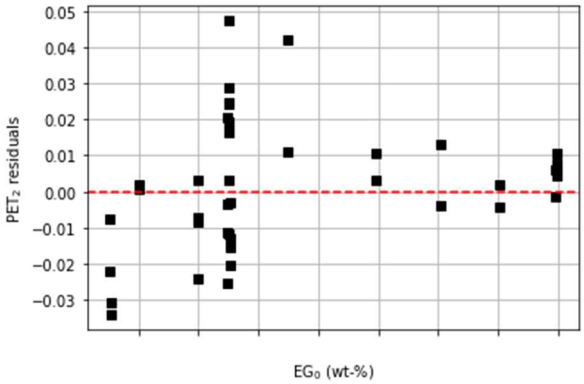

Figure 4-32: PET_2 residuals VS EG_0 for the proposed formalism.

5 Conclusions and future perspectives

5.1 Conclusions

The current thesis had two main objectives. The first objective was to perform a kinetic study of a synthetic PET (re)polymerisation system involving pure BHET and EG as reactants and Sb_2O_3 as catalyst, in order to observe the effect of a series of reaction parameters, *i.e.*, $BHET_0$:EG_0, [Sb], temperature and precursor of Sb on the rate of reaction.

The second objective was to create a mathematical model in order to predict the behaviour of the system studied experimentally and investigate the conditions in which EG inhibits the catalytic activity of Sb, if at all. The parameters of the model were tuned based on the experimental results and, in order to account for the catalytic activity of Sb, three different activity formalisms were attempted: two were found in literature and one was proposed based on the experimental results.

First, the obtained experimental results were analysed in order to observe the effects of the abovementioned parameters on the rate of reaction. It was clear that the rate of reaction varied directly proportional to [Sb], as it would be expected from catalysed kinetics. The effect of $BHET_0$:EG_0 was not very clear, because it required the comparison between the progress of the equilibrium reaction in reactors with different initial compositions, which greatly affect the rate of reaction. The effect of the precursor of Sb on the rate of reaction was not clear either, and the uncertainty in the measurement of the mass of powdered Sb_2O_3 and the possible limit of solubility of Sb_2O_3 in the reaction medium were thought to have played a key role.

Just by analysing the experimental results, it was not possible to state clearly whether or not EG inhibited the catalytic activity of Sb, due to the unclear effect that $BHET_0$:EG_0 had on the rate of reaction. By varying $BHET_0$:EG_0, not only the degree of the possible inhibition of the catalytic activity of Sb by EG was changed, due to varying EG_0, but also the driving force of the reaction was changed. The combination of both of these effects, added to experimental and analytical uncertainty, made it difficult to draw conclusions from the effect of $BHET_0$:EG_0. It was visible that the rate of reaction was noticeably lower when EG_0 was equal to XX wt-%, but in order to ascertain whether or not EG presents an inhibitory effect and to which extent, it was necessary to proceed to the modelling part of the work.

Based on the experimental results, the different parameters of a mathematical model for the reactor were tuned. For all three formalism, values of k_{ref}^{th}, k_{ref}^{cat} and E_a could be estimated with good precision. For the Hovenkamp formalism, one additional parameter, k_{inh}, was also tuned. Finally, when using the formalism proposed in the current work, three additional parameters, α, β and γ were tuned.

The tuned value of E_a of 96±6 kJ/mol was considerably close to that found by Hovenkamp (88 kJ/mol) and that found by El-Toufaili *et al.* (75±5 kJ/mol) [21] [15]. It should be noted that the system studied in the three cases were not the same, *i.e.*, Hovenkamp studied the esterification reaction in a model system, El-Toufaili *et al.* studied polycondensation and, in the current work, short-chain oligomerisation was studied. However, in all three cases, Sb_2O_3 was used as catalyst. In the current work, the main

objective was not to find E_a, and its estimation was done based on only two sets of experimental results (at 170ºC and 190ºC). In order to obtain a better estimation of E_a the reaction should have been carried out over a wider range of temperatures).

By applying the tuned formalisms to the reactor model, it was possible to see clear trends. The Yamada formalism normally showed a good fitting to the experimental results (R^2 above 0.95) when EG_0 was below *ca.* 25 wt-%. The Hovenkamp formalism, on the other hand, normally showed a much superior fitting than Yamada to the experimental results when EG_0 was above and equal to *ca.* 25 wt-%, but a slightly inferior fitting for EG_0 below that value. This due the fact that the Hovenkamp formalism considers that EG inhibits the catalytic activity of Sb, while the Yamada formalism does not. Additionally, the additional parameter k_{inh} was tuned using a different range of experimental results than k^{cat}, *i.e.*, the former was tuned using sets of experimental results at high EG_0, while the latter was tuned using sets of experimental results at low EG_0. This could have also caused the observed behaviour of the Hovenkamp formalism. Furthermore, k^{th}, k^{cat} and E_a were not refitted in the Hovenkamp formalism.

The formalism proposed in the current work also considers that EG inhibits the catalytic activity of Sb, but it proposes a more complex correlation between k and [Sb] than both formalisms from literature. The additional three parameters proposed and tuned in this formalism allowed for a good prediction of the experimental results for all ranges of BHET:EG and [Sb] studied, meaning that its range of applicability is superior to that of both formalisms from literature. The values of R^2 obtained using the proposed formalism are almost always superior to the highest value of R^2 from among the two formalisms from literature.

By comparing the results from the modelling work with the tuned parameters to the experimental results, it is possible to infer that inhibition of the catalytic activity of Sb by EG does take place in the current system, and that it is mostly visible when EG_0 is above *ca.* 25 wt-%, given that this is the value above which the Yamada formalism, which does not account for the inhibitory effect, starts to show significant deviation. Furthermore, this inhibition is directly proportional to EG_0. The Yamada formalism shows a good fitting to the experimental results when the effect of this inhibition is negligible, whilst the Hovenkamp shows a good behaviour when EG_0 is high enough so that its inhibitory effect is no longer negligible. The proposed formalism presents a good prediction of the experimental results for all ranges of EG_0., but it can only be used when Sb is present inside the reactor.

Bibliography

[1] S. Mandal and A. Dey, “PET Chemistry,” *Recycling of Polyethylene Terephthalate Bottles,* pp. 1-22, 2019.

[2] I. Tiseo, “Global demand for polyethylene terephthalate 2010-2030,” Statista, 22 April 2021. [Online]. Available: https://www.statista.com/statistics/1128658/polyethylene-terephthalate-demand-worldwide/. [Accessed 9 May 2022].

[3] I. Tiseo, “Global PET packaging consumption shares 2019, by end-use sector,” Statista, 21 June 2021. [Online]. Available: https://www.statista.com/statistics/858624/global-polyethylene-terephthalate-consumption-distribution-by-end-use/. [Accessed 9 May 2022].

[4] I. Tiseo, “Global PET bottle production 2004-2021,” Statista, 27 January 2021. [Online]. Available: https://www.statista.com/statistics/723191/production-of-polyethylene-terephthalate-bottles-worldwide/. [Accessed 9 May 2022].

[5] Dayamanti and H.-S. Wu, “Strategic Possibility Routes of Recycled PET,” *Polymers,* vol. 13, no. 9, 2021.

[6] EPBP, “How to keep a sustainable PET recycling industry in Europe,” [Online]. Available: https://www.epbp.org/. [Accessed 9 May 2022].

[7] Environmental Protection Agency, “AP-42: Compilation of Air Emissions Factors,” in *Chapter 6: Organic Chemical Process Industry*, 1995, pp. 1-13.

[8] Ullmann's Encyclopedia of Industrial Chemistry, 7 ed., vol. 40, Wiley-VCH, 2011.

[9] J. Fremondeau, “Le Polytéréphtalate d’éthylène (PET),” 10 May 2017. [Online]. Available: https://ramenetessciences.wordpress.com/2017/05/10/le-polyterephtalate-dethylene-pet/. [Accessed 5 September 2022].

[10] F. Awaja and D. Pavel, “Recycling of PET,” *European Polymer Journal,* vol. 41, pp. 1453-1477, 2005.

[11] S. H. Park and S. H. Kim, “Poly (ethylene terephthalate) recycling for high value added textiles,” *Fashion and Textiles,* 2014.

[12] H. Goh, A. Salmiaton, N. Abdullah and A. Idris, “Time, Temperature and Amount of Distilled Water Effects on the Purity and Yield of Bis(2-hydroxyethyl) Terephthalate Purification System,” *Bulletin of Chemical Reaction Engineering & Catalysis,* vol. 10, no. 2, pp. 143-154, 2015.

[13] A. Sheel and D. Pant, “Chemical Depolymerization of PET,” *Recycling of Polyethylene Terephthalate Bottles,* pp. 60-84, 2019.

[14] J. Huang, D. Yan, H. Dong, F. Li, X. Lu and J. Xin, “Removal of trace amount impurities in glycolytic monomer of polyethylene terephthalate by recrystallization,” *Journal of Environmental Chemical Engineering,* vol. 9, no. 5, 2021.

[15] F.-A. El-Toufaili, G. Feix and K.-H. Reichert, “Mechanistic Investigations of Antimony-Catalyzed Polycondensation in the Synthesis of Poly(ethylene terephthalate),” *Journal of Polymer Science: Part A: Polymer Chemistry,* vol. 44, p. 1049–1059, 2006.

[16] T. Yamada, “Effect of Diantimony Trioxide on Direct Esterification between Terephthalic Acid and Ethylene Glycol,” *Journal of Applied Polymer Science,* vol. 37, pp. 1821-1835, 1989.

[17] J.-W. Chen and L.-W. Chen, “The Kinetics of Diethylene Glycol Formation from Bishydroxyethyl Terephthalate with Antimony Catalyst in the Preparation of PET,” *Journal of Polymer Science: Part A: Polymer Chemistry,* vol. 37, pp. 1797-1803, 1999.

[18] T. H. Shah, J. I. Bhatty and G. A. Gamlen, “Aspects of the chemistry of poly(ethylene terephthalate): 5. Polymerization of bis(hydroxyethyl)terephthalate by various metallic catalysts,” *Polymer,* vol. 29, no. 9, pp. 1333-1336, 1984.

[19] S. B. Maerov, “Influence of Antimony Catalysts with Hydroxyethoxy Ligands on Polyester Polymerization,” *Journal of Polymer Science: Polymer Chemistry Edition,* vol. 17, pp. 4033-4040, 1979.

[20] B. Duh, “Effect of antimony catalyst on solid-state polycondensation of poly(ethylene terephthalate),” *Polymer,* vol. 43, pp. 3147-3154, 2002.

[21] S. G. Hovenkamp, “Kinetic Aspects of Catalyzed Reactions in the Formation of Poly(ethy1ene terephthalate,” *Journal of Polymer Science: Part A-1,* vol. 9, 1971.

[22] *Chapter 3: Reaction Kinetics,* 2004.

[23] T. K. Harris and M. M. Keshwani, Methods in Enzymology, 2 ed., vol. 463, 2009, pp. 57-71.

[24] D. P. Minh, T. J. Siang, D.-V. N.Vo, T. S. Phan, C. Ridart, A. Nzihou and D. Grouset, Hydrogen Supply Chains, Academic Press, 2018, pp. 111-166.

[25] A. D. Padsalgikar, Plastics in Medical Devices for Cardiovascular Applications, William Andrew, 2017.

[26] M. Blaber and T. Neils, "7.11 Gibbs Free Energy and Equilibrium," 5 Junho 2019. [Online]. Available: https://chem.libretexts.org/Courses/Grand_Rapids_Community_College/CHM_120_-_Survey_of_General_Chemistry/7%3A_Equilibrium_and_Thermodynamics/7.11%3A_Gibbs_Free_Energy_and_Equilibrium. [Accessed 5 Setembro 2022].

[27] Q. S. Y. Yeung, C. M. Briton-Jones and G. C. C. Tjer, "The Efficacy of Test Tube Warming Devices Used," *Journal of Assisted Reproduction and Genetics,* vol. 21, no. 10, pp. 355-360, 2004.

[28] Thermo Scientific™, "Thermo Scientific™ Digital Dry Baths/Block Heaters," [Online]. Available: https://www.fishersci.com/shop/products/digital-dry-bath-block-heater/88870001. [Accessed 26 Julho 2022].

[29] G. L. Foutch and A. H. Johannes, Encyclopedia of Physical Science and Technology, vol. 3, Reference Work, 2003.

[30] Lenz Laborglasinstrumenten, "Information about DURAN®," [Online]. Available: https://www.lenz-laborglas.de/en/technical-details/information-about-duran.html. [Accessed 26 Julho 2022].

[31] DWK Life Sciences, "DURAN® Original GL 45 Laboratory Bottle, clear, with high temperature resistant screw cap (PBT, red) and pouring ring (ETFE, red)," [Online]. Available: https://www.dwk.com/duran-original-gl-45-laboratory-bottle-clear-with-high-temperature-resistant-screw-cap-pbt-red-and-pouring-ring-etfe-red. [Accessed 26 Julho 2022].

[32] IKA, "Stirring," [Online]. Available: https://www.ika.com/en/Applications/Stirring-appl-2.html#:~:text=Stirring%20allows%20for%20the%20homogenization,the%20speed%20of%20chemical%20reactions.. [Accessed 26 Julho 2022].

[3 3] M. Loos, “Processing of Polymer Matrix Composites Containing CNTs,” in *Carbon Nanotube Reinforced Composites*, William Andrew, 2015.

[3 4] D. Rossouw, “Point Temperature Measurements,” in *Application of Thermo-Fluidic Measurement Techniques*, Butterworth-Heinemann, 2016.

[3 5] DBpedia, “About: Sparging (chemistry),” [Online]. Available: https://dbpedia.org/page/Sparging_(chemistry). [Accessed 27 Julho 2022].

[3 6] P. K. Deb, S. F. Kokaz, S. N. Abed, A. Paradkar and R. K. Tekade, “Pharmaceutical and Biomedical Applications of Polymers,” in *Basic Fundamentals of Drug Delivery*, Academic Press, pp. 203-267.

[3 7] H. Engelhardt and G. Ahr, “Optimization of efficiency in size-exclusion chromatography,” *Journal of Chromatography A,* vol. 282, pp. 385-397, 1983.

[3 8] L. M. Martínez, “Size exclusion chromatography columns,” 14 Junho 2018. [Online]. Available: https://www.sepmag.eu/blog/size-exclusion-chromatography-columns. [Accessed 7 September 2022].

[3 9] D. W. Watson, “Optimizing Size-Exclusion Chromatography (SEC) for Biologics Analysis,” 1 Março 2018. [Online]. Available: https://www.chromatographyonline.com/view/optimizing-sec-biologics-analysis-0. [Accessed 7 Setembro 2022].

[4 0] Shodex™, “Lesson 6: Detectors for HPLC,” [Online]. Available: https://www.shodex.com/en/kouza/f.html#!. [Accessed 7 Setembro 2022].

[4 1] B. Raut, “High-Pressure Liquid Chromatography (HPLC), Principle, Instruments, and Applications,” 8 October 2021. [Online]. Available: https://chemistnotes.com/organic/high-pressure-liquid-chromatography-hplc-principle-instruments-and-applications/#:~:text=in%20a%20mixture.-,Principle%20of%20HPLC%20(High%2DPerformance%20liquid%20Chromatography),phase%20used%20in%20the%20separation. [Accessed 8 September 2022].

[4 2] Creative Proteomics, “The Principle of High-Performance Liquid Chromatography (HPLC),” [Online]. Available: https://www.creative-proteomics.com/pronalyse/the-principle-of-high-performance-liquid-chromatography-hplc.html. [Accessed 8 September 2022].

[4 3] J. Böttcher, M. Margraf and K. Monks, “HPLC Basics – principles and parameters,” KNAUER Wissenschaftliche Geräte GmbH, [Online]. Available:

https://www.knauer.net/Application/application_notes/VSP0019_HPLC%20Basics%20-%20principles%20and%20parameters_final%20-web-.pdf. [Accessed 8 September 2022].

[44] Merck, "Method development & optimization," [Online]. Available: https://www.sigmaaldrich.com/deepweb/assets/sigmaaldrich/marketing/global/documents/201/658/dicas-de-desenvolvimento-de-metodo-e-otimizacoes.pdf. [Accessed 8 September 2022].

[45] R. W. Stevenson and H. R. Nettleton, "Polycondensation Rate of Poly(ethylene Terephthalate) . I. Polycondensation Catalyzed by Antimony Trioxide in Presence of Reverse Reaction," *Journal of Polymer Science: Part A-1,* vol. 9, 1968.

[46] G. Challa, "The formation of polyethylene terephthalate by ester interchange. II. The kinetics of reversible melt-polycondensation," *Die Makromolekulare Chemie,* vol. 38, no. 1, pp. 123-137, 1960.

[47] K. Tomita, "Studies on the formation of poly(ethylene terephthalate): 6. Catalytic activity of metal compounds in polycondensation of bis(2-hyd roxyethyl) terephthalate," *Polymer,* vol. 17, no. 3, pp. 221-224, 1976.

[48] P. Gielen, "Cumapol builds pilot plant for chemical PET recycling," Agro&Chemistry, 26 Juin 2018. [Online]. Available: https://www.agro-chemistry.com/articles/cumapol-builds-pilot-plant-for-chemical-pet-recycling/. [Accessed 11 Juillet 2022].

[49] K. Tomita, "Studies on the formation of poly(ethylene terephthalate): 1. Propagation and degradation reactions in the polycondensation of bis(2-hyd roxyethyl) terephthalate," *Polymer,* vol. 14, pp. 50-54, 1973.

[50] IFP Energies nouvelles, "Contribution of Chemistry to Plastics Recycling," [Online]. Available: https://www.ifpenergiesnouvelles.com/innovation-and-industry/our-expertise/climate-environment-and-circular-economy/plastics-recycling/our-solutions. [Accessed 11 Juillet 2022].

[51] R. Rulkens and C. Koning, Polymer Science: A Comprehensive Reference, Elsevier, 2012.

Annex A – Chemical structures of selected species

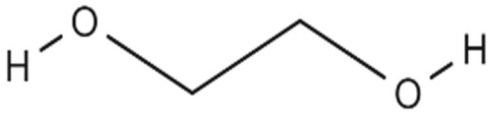

Fig. Annex 1: EG.

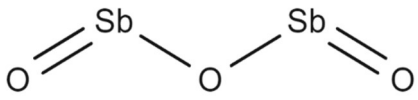

Fig. Annex 2: Sb_2O_3.

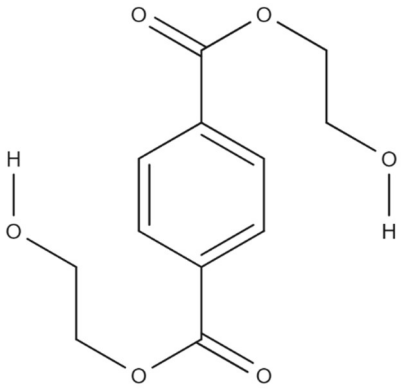

Fig. Annex 3: BHET.

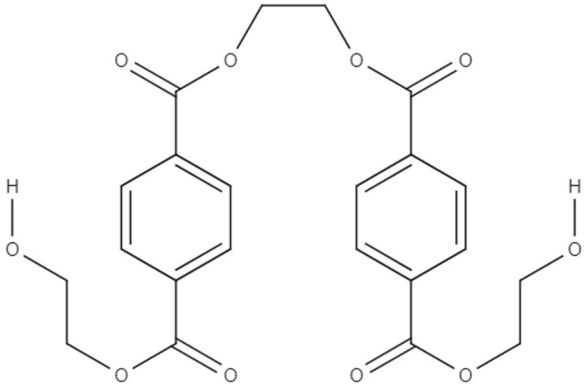

Fig. Annex 4: PET_2.

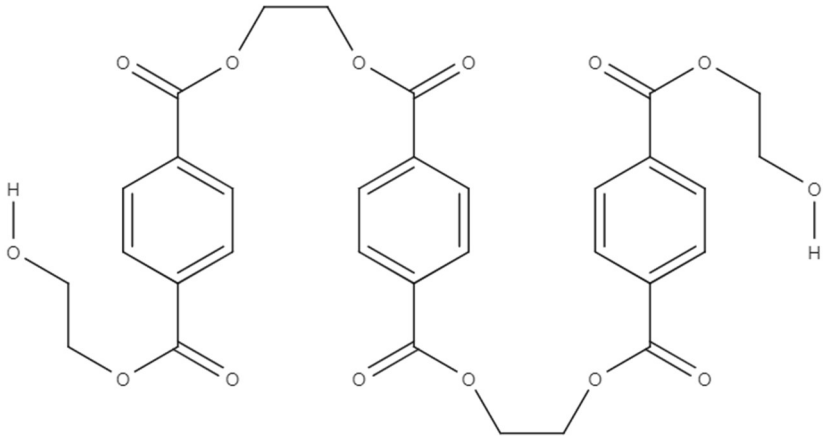

Fig. Annex 5: PET_3.

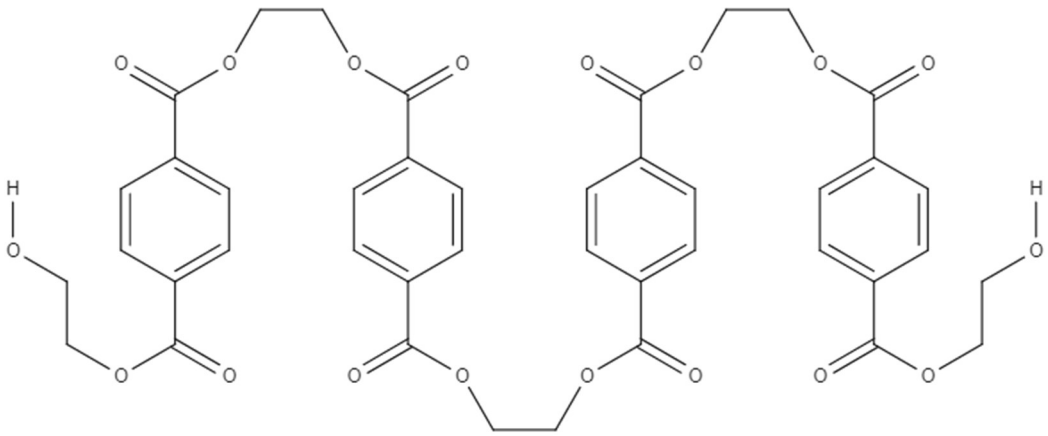

Fig. Annex 6: PET_4.